Available online at www.sciencedirect.com
ScienceDirect
Trans. Nonferrous Met. Soc. China 31(2021) 3255−3280
Transactions of Nonferrous Metals Society of China
www.tnmsc.cn

Semi-solid processing of aluminum and magnesium alloys: Status, opportunity, and challenge in China

Gan LI[1], Wen-ying QU[1], Min LUO[1], Le CHENG[1], Chuan GUO[1], Xing-gang LI[1,2], Zhen XU[1], Xiao-gang HU[1,2], Da-quan LI[3], Hong-xing LU[1], Qiang ZHU[1]

1. Department of Mechanical and Energy Engineering, Southern University of Science and Technology, Shenzhen 518055, China;
2. Academy for Advanced Interdisciplinary Studies, Southern University of Science and Technology, Shenzhen 518055, China;
3. GRIMAT Engineering Institute Co., Ltd., Beijing 101407, China

Received 14 September 2021; accepted 8 November 2021

Abstract: Owing to its low cost, short process and low energy consumption, semi-solid processing (SSP) of aluminum (Al) and magnesium (Mg) alloys has been considered as a competitive approach to fabricate complicated components with excellent performance. Over the past decade, significant progress has been achieved in deeply understanding the SSP process, the microstructure and performance of the fabricated components in China. This paper starts with a retrospective overview of some common slurry preparation methods, followed by presenting the performance and the underlying mechanisms of SSP fabricated alloys. Then, the mainstream opinions on the microstructure evolution and rheological flow behavior of semi-solid slurry are discussed. Subsequently, the general situation and some recent examples of industrial applications of SSP are presented. Finally, special attention is paid to the unresolved issues and the future directions in SSP of Al and Mg alloys in China.

Key words: semi-solid processing; aluminum alloys; magnesium alloys; slurry preparation; numerical modeling; performance; industrial applications

1 Introduction

As the two lightest metal structural materials of commercialization, aluminum (Al) and magnesium (Mg) alloys exhibit excellent specific strength, high specific stiffness, superior thermal conductivity, good recyclability and natural availability, thus obtaining extensive applications in many sectors, such as automobile, aerospace and 3C products [1−4]. In recent years, the strong demand for lightweight structure and function integration components with high performance and low cost is increasingly promoting, which poses great challenges to the properties of Al and Mg alloys. To grapple with this long-term issue, it is significantly essential to further develop Al and Mg alloys by designing new alloys or optimizing their processing routes to satisfy the requirements of the market.

Currently, the conventional processing routes of Al and Mg alloys primarily include liquid forming and forging [5,6]. Liquid forming mainly consists of sand casting, squeeze casting, gravity casting, high pressure die casting (HPDC) and so forth. The HPDC process has been widely explored because it can provide vast advantages in terms of superior metallurgical quality, high productivity and

Corresponding author: Hong-xing LU, Tel: +86-755-88018144, E-mail: luhx@sustech.edu.cn;
Qiang ZHU, Tel: +86-755-88018131, E-mail: zhuq@sustech.edu.cn
DOI: 10.1016/S1003-6326(21)65729-1

easy realization of automatic production. However, it cannot be neglected that the structural integrity of the parts processed by HPDC is always plagued by inherent defects like shrinkage, pores and hot cracking. In addition, these parts normally cannot undergo means of heat treatment to further enhance their properties due to the appearance of subsurface blisters. Thus, these parts are not sufficient for some structural applications required in modern industries. Although the forged parts show good relative density and mechanical properties, the high production cost and low efficiency limit their wide applications seriously. In the recent years, metal additive manufacturing (AM), such as direct energy deposition (DED) and laser powder bed fusion (L-PBF), has attracted considerable interest in both academic and industrial world as it can rapidly build highly complex geometric and high-performance parts without using molds [7−9]. But, currently a very limited number of Al and Mg alloys are regarded as "easily printed and quality deposit", and the feedstock (usually the micron-sized powders) and processing costs are also relatively expensive [10−12]. Fortunately, compared with the above-mentioned processes, semi-solid processing (SSP) benefiting from both casting and forging displays a bright prospect to commercially produce high-quality components with low cost and short process.

The SSP, which employs the semi-solid slurry with non-dendritic (spherical) grains as the feedstock, is an advanced near-net-shape forming technology. The special slurry, the state of which is temperature- and time-dependent, ensures that the alloy displays the thixotropic behavior under shear [13−15]. The slurry can fill the mold in a more controllable and non-turbulent manner to avoid the common gas entrapment defects that usually found in classic casting and to obtain near fully dense parts that can be further strengthened through suitable heat treatment [16−19]. Besides, the relatively low forming temperature could reduce the thermal shock to the die and lessen the solidification shrinkage, ensuring near-net shape forming and high surface quality [20−22].

After the development of almost half a century, the focus of SSP has gradually transformed from basic research to key technology and application research. This requires not only a profound knowledge of the process itself, but also the evolution mechanism of microstructure and the final performance of the fabricated components. Significant progress in understanding the SSP of Al and Mg alloys has been made primarily due to the industry upgrading and the strong demand of the market in China over the past decade. Until now, SSP has been successfully utilized to manufacture automobile steering arm, brake caliper, 5G base station filter, and other components, exhibiting favorable prospects for engineering development and promotion. Therefore, it is of vital importance to give a comprehensive overview of SSP of Al and Mg alloys.

In this paper, we will first discuss the semi-solid slurry preparation process in China, followed by the performance of SSP fabricated parts. Afterwards, the research status of microstructure evolution and flow behavior mechanism of slurry in SSP will be summarized and discussed. The general situation and some examples of successful applications of SSP in China are presented subsequently. Finally, we will highlight the unresolved problems and put forward the future developmental direction in this frontier research field.

2 Slurry preparation methods

2.1 Common methods in China

Preparation of the semi-solid slurry with non-dendritic grains as the feedstock is the first step and prerequisite for SSP [23−25]. The main aim is to prepare high-quality slurry with homogeneously dispersed and spherical microstructure, which exerts marked effect on the properties of the components. Under the economic pressure of reducing the production cost and time as much as possible, the attention of SSP has gradually converted from thixoforming to rheoforming [26−29]. So far, around 30 types of methods for slurry preparation have emerged based on various solidification conditions. As summarized in Table 1, there are nearly 20 types of methods that consist of both self-developed and introduced methods in China.

These slurry preparation methods can be grouped into three subsets: (1) agitation/stirring, such as mechanical stirring and electromagnetic stirring, (2) regulation of grain nucleation and growth process, and (3) integration of (1) and (2).

In order to achieve superior stability of growing spheroids, ample nuclei in the early stage of solidification should be generated in these subsets [79]. It can be observed in Table 1 that almost all the methods can prepare slurry with average particle size (APS) less than 100 μm and shape factor (S_F) over 0.5, suggesting that these methods could theoretically generate eligible slurry for further forming. But, most of the self-developed methods in China are still in the experimental stage despite some industrial trials. From the perspective of the application, cost, efficiency, product quality

Table 1 Summary of slurry preparation methods developed and adopted in China

Process	Affiliation	Some commonly used Al and Mg alloys
Indirect ultrasonic vibration (IUV)	Huazhong University of Science and Technology	356 (f_s=0−0.22) [30], 5083 (f_s=0−0.23) [31], SiC_p/Al [32], Mg−Zn−Y [33]
Low superheat pouring with a shear field (LSPSF)	Nanchang University	356 (f_s=0.4) [34], 2024 [35], 7075 [36], AZ91 [37]
Internal rapid cooling stirring process (IRCSP)	Nanchang University	AZ91D (f_s=0−0.32) [38]
Self-inoculation method (SIM)	Lanzhou University of Technology	356 (f_s=0.27) [39], 2024 [40], 6061 (f_s≈0.4) [41], AM60 [42]
Forced convection stirring (FCS)	University of Science and Technology Beijing	356 [43], A380 [44], 7075 (f_s≈0.1) [45], AZ91D [43]
Inverted cone-shaped pouring channel (ICSPC)	University of Science and Technology Beijing	7075 (f_s≈0.15, 0.46) [46,47]
Annular electromagnetic stirring (A-EMS)	General Research Institute for Non-ferrous Metals (GRINM)	357 [48], 7075 [49]
Serpentine channel pouring (SCP)	University of Science and Technology Beijing	356 (f_s≈0.5) [50,51], A380 [52], 7075 (f_s≈0.2) [53]
Pulsed magnetic field process (PMF)	Nanchang Hangkong University	356 (f_s≈0.2) [54], 2024 [55]
Rotate casting method (RCM)	Harbin Institute of Technology	7A09 [56]
Melt spreading and mixing technique (MSMT)	General Research Institute for Non-ferrous Metals (GRINM)	Al6.5Si [57]
Helical curve duct (HCD)	Nanchang University	356 [58], 6063 [59], 7075 [59]
Air-cooled stirring rod device (ACSR)	University of Science and Technology Beijing	Al8Si [60], Al−Si−Fe−Mg−Sr [61], Al7.5Si0.8Fe [62], 7075
Distributary-confluence channel (DCC)	University of Science and Technology Beijing	356 (f_s≈0.26−0.48) [63], A380 [63], AZ91D [63]
Enthalpy control process (ECP)	Southern University of Science and Technology	7075 (f_s≈0.4) [23]
Limited angular oscillation (LAO)	Nanchang University	AZ91 [37]
†Gas induced semi-solid (GISS)	Massachusetts Institute of Technology	356 (f_s≈0−0.21) [64], 383 [65], 7075 (f_s≈0.14−0.27) [27]
†Swirled enthalpy equilibration device (SEED)	Alcan / STAS Inc.	356 (f_s≈0.3−0.45) [66], 206 [67], 7075 (f_s≈0.42−0.55) [68]
†New rheocasting (NRC)	UBE Industries	356 [69,70], AZ71 [71]
†Rapid slurry formation (RSF/RheoMetal)	Jonkoping University	356 (f_s≈0.28−0.35) [72], Al7Si [73], Al8Si [74], 6063 [74]
†Cooling slope (CS)	UBE Industries	356 [75], A380 [76], A390 [77], 6082 [78]

† Introduced methods

and stability of the slurry preparation process have always been the critical issues of concern. For instance, the air-cooled stirring rod (ACSR) process, a relatively novel method invented by QI et al [80] has gained increasing attention across both academic and industrial sectors. It can be used to prepare excellent slurry with the solid fraction (f_s) of 55%, the APS of 38 μm and the shape factor of 0.86, as shown in Fig. 1. Recently, their work showed that only 25 s was required to produce 32 kg of the Al alloy slurry using this powerful method [61]. Although only a handful of these self-developed methods in China have been cosmically employed in industrial production, these studies and attempts have accumulated valuable experience for the slurry preparation.

On the other side, some slurry preparation methods that have demonstrated the potential of mass production have been introduced to China to realize engineering applications, like swirled enthalpy equilibration device (SEED) and gas induced semi-solid (GISS). The SEED process, proposed by the Alcan (now Rio Tinto Alcan, Canada) at the end of the 1990s, is a simple but efficient slurry preparation method that can produce high mass slurry with a high solid fraction (normally 35%−55%) [81,82]. This method was introduced to China in the early 2010s, and since then many production lines have been established. The development and some recent innovations of the SEED process in China will be reviewed in detail in the following section.

2.2 Development of SEED process

Figure 2 presents the SEED unit, crucibles of various sizes and the corresponding slurry. The principle is based on achieving rapid and controlled thermal equilibrium between a metallic crucible, the molten alloy and the environment by using the proper processing parameters such as pouring temperature, crucible size and swirled duration. This method includes the following three steps: (1) titling the crucible and pouring the molten alloy, (2) straightening the crucible and swirling it eccentrically at a certain speed for a certain duration, and (3) finally demolding and transferring

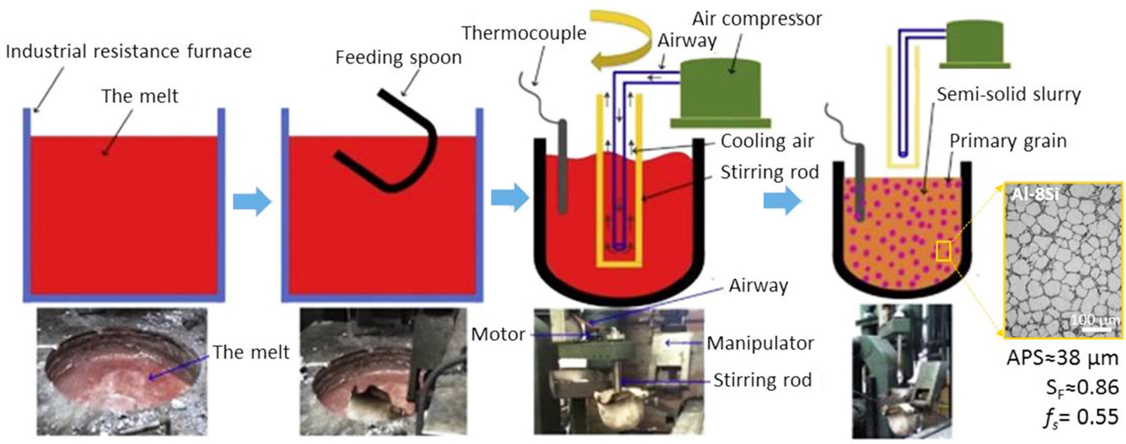

Fig. 1 Schematic diagrams and physical maps for slurry preparation of ACSR process (The inserted OM image reveals quenched microstructure of Al−8Si alloy slurry) [62,80]

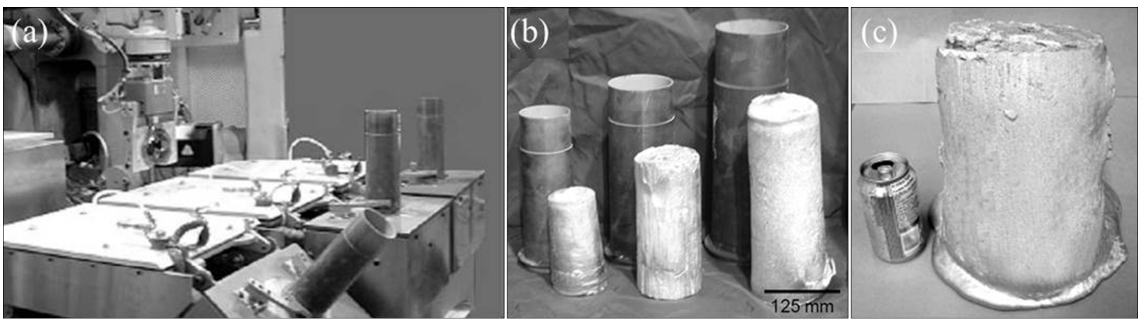

Fig. 2 SEED unit (3 modules) (a), crucible and slurry size (~2 to 10 kg) (b), and large A356 Al alloy slurry of ~18 kg (c) [83]

to forming [84]. As one of the few methods that can produce slurry with a high solid fraction, it has developed to industry level [22,85−87].

To further improve the efficiency of SEED process, LUO et al [88] conducted a secondary development, mainly comprising in-depth understanding the underlying thermodynamics and kinetic mechanisms of solidification process during the slurry preparation, optimizing the process and equipment (Fig. 3(a)). They concluded that the heat-transfer coefficient of the crucible-air interface and the slurry radius were the critical factors for decreasing the radial temperature difference of the slurry. Furthermore, they also established an accurate model to comprehend the relationship between temperature distribution along the slurry radius and parameters at a quasi-steady state [89]. The modified SEED process can noticeably decrease the radial temperature gradient of the A201 alloy melt because of the slow cooling rates, facilitating more uniform slurry and more spherical microstructures, as illustrated in Fig. 3(b). In addition, the modified process can also prepare excellent slurry for the high-strength wrought Al alloys even though they have narrow processing window resulting from the long solidification temperature interval. As demonstrated in Fig. 3(c), the comparison of internal defects in between the original and modified SEED processes also showed that few pores were detected in the 7050 Al alloy part manufactured by the modified process.

Figure 4 shows the temperature distribution, rheological state and morphology of 7108 alloy slurry produced by the conventional and modified SEED processes. The uniformity of temperature distribution was obviously improved and the

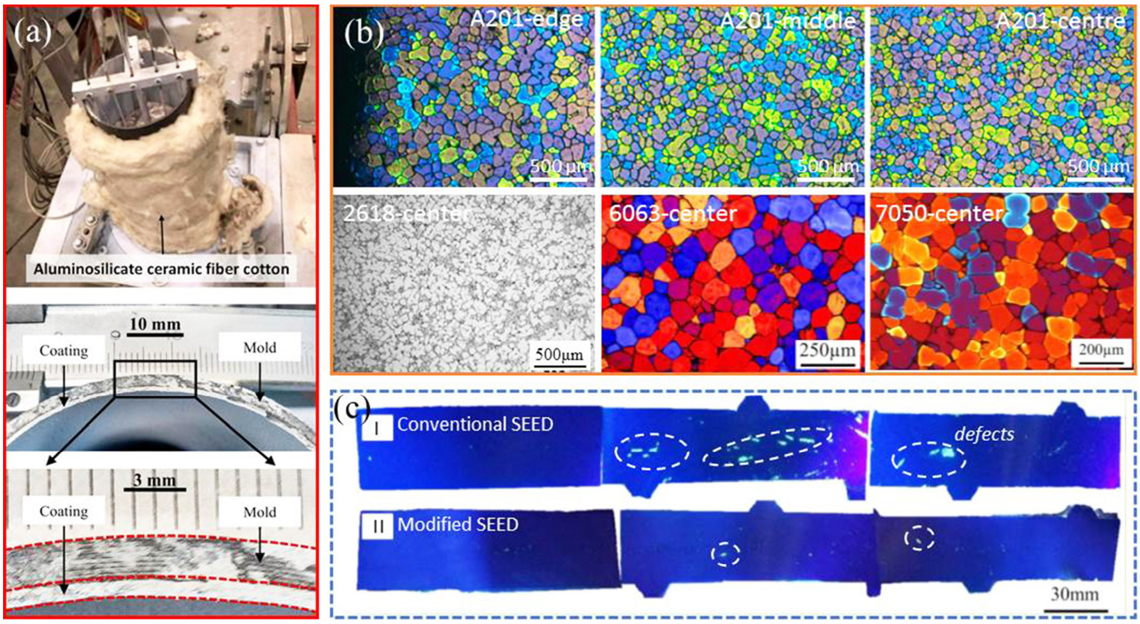

Fig. 3 Modified SEED process (photograph of ceramic fiber cotton on external mold surface and layer boron nitride coating on internal mold surface) (a) [89,90], A201, 2618, 6063 and 7050 Al alloy slurries at different position (b) [87,90], and results of internal defects of 7050 parts (c) [90]

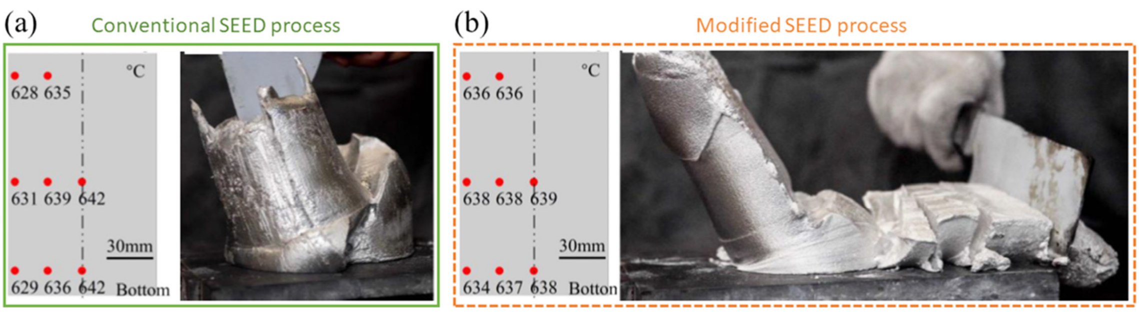

Fig. 4 Temperature distribution, rheological state and morphology of 7108 alloy slurry produced by conventional (a) and modified (b) SEED processes [90]

temperature difference reduced from ~14 to ~5 °C after optimizing the process, indicating that the difference of solid fraction and viscosity in different regions was quite small. This is conducive to enhancing the performance of the final parts. They also uncovered the influence of the heat exchange process on the microstructure of the slurry, concluding that the grain refinement can be achieved by increasing the heat exchange rate at the early stage of the SEED process. In addition, the influence of grain refiner and pouring temperature on the microstructure of 357 slurry prepared by the SEED process was also investigated. It was found that the fine and round microstructure could be processed at low pouring temperature, whereas the refiner had no significant impact on the microstructure at low casting temperature [25,91,92].

3 Performance of SSP fabricated materials

With the increasing popularity of SSP, it is significantly essential to assess the feasibility of its use for structure components through performance tests. The microstructural features caused by the distinctive slurry may improve the performance. In recent decades, a considerable number of investigations have been performed to study the excellent performance of the SSP fabricated materials in terms of tensile behavior, creep resistance, fatigue performance, wear resistance, corrosion resistance and so forth [93−100]. This section will mainly cover the tensile behavior and thermal conductivity, which have received researchers' much attention in the literatures.

3.1 Tensile behavior

In general, SSP of Al and Mg alloys is commonly realized by a sound combination of slurry preparation and a range of processing methods, such as rolling, squeeze casting (SC), high pressure die casting (HPDC) and thixomolding (for Mg alloys). In general, the static strength depends on the relative density as well as the microstructure formed during SSP. Hence, as compared to parts processed by classical routes (i.e., casting), the reduced defects and fine microstructure offered by SSP primarily result in improved tensile strength and elongation.

Some of the tensile properties of four types of popular alloys (i.e., A356 Al, 7075 Al, AZ91 Mg and AZ91D Mg) from the literatures are shown in Tables 2−3 and Fig. 5. It can be clearly observed that the SSP fabricated alloys reveal better performance than their conventionally processed counterpart in the as-fabricated condition, indicating the effectiveness of the SSP. The reason for the increment of mechanical properties is primarily twofold. The first is the refinement of the α-Al/α-Mg. It has been proved that fine spherical primary particles are conducive to mechanical properties while the refinement of α_2-Al/α_2-Mg within the eutectic structure is a critical factor determining the yield strength of alloys [64]. Hence, grain refinement causes an increase in both yield strength (YS) and ultimate tensile strength (UTS) due to the Hall-Petch effect. The second is the high relative density resulting from less entrapped air and shrinkage porosity. It is widely accepted that porosity is detrimental to mechanical properties and one of the key targets of processing structural components is reducing internal porosity. For SSP, the unique slurry exhibits distinctive pseudo-plasticity and thixotropy, dramatically reducing air entrapment during filling because of a higher viscosity compared with the liquid metal [14,17]. The lower forming temperature during SSP also brings about lower solidification shrinkage, which can reduce defects and obtain near fully-dense parts.

The mechanical properties are noticeably improved for these heat-treatable alloys as the porosity is very low. As exhibited in Fig. 5, there is a remarkable increase in UTS after heat treatment. The objective of any heat treatment procedure is to modify the microstructure to alter the properties to suit its function in an application [10]. However, the heat treatment has mostly been limited to the application of traditional routes to the SSP fabricated materials. These traditional procedures have been specifically tailored for the different microstructures that are processed by conventional processes. Accordingly, designing or revising a heat treatment procedure for SSP should consider both the starting and resultant microstructures.

On the other hand, it is also worth mentioning that the SSP fabricated materials also display better-elevated temperature properties. For example, QI et al [62] found that the Rheo-HPDC Al−Si−Fe alloy

Table 2 Mechanical properties of A356 and 7075 Al alloys fabricated by various SSP processes as compared to conventionally processed alloys in different conditions

Alloy	Process	HT	UTS/MPa	YS/MPa	EL/%	Hardness (HV)	Ref.
A356	HPDC	AF	223	−	4.28	−	[30]
	IUV Rheo-HPDC	AF	254	−	7.5	−	[30]
	IUV Rheo-SC	T6	338	227	8	126	[101]
	GISS Rheo-HPDC	AF	235	−	7.4	−	[65]
	GISS Rheo-HPDC	T6	312	277	7.6	−	[102]
	GISS Rheo-HPDC	T6	305	272	9.8	−	[102]
	ISCT Rheo-HPDC	AF	242	−	12.5	73	[103]
	HPDC	AF	221±17	135±6	3.7±1.4	71±9	[43]
	FCS Rheo-HPDC	AF	260±6	181±4	8.4±0.5	79±5	[43]
	FCS Rheo-HPDC	T4	275±8	166±6	13.6±1	82±7	[43]
	FCS Rheo-HPDC	T6	323±10	232±7	7.3±0.8	93±8	[43]
	GDC	T6	315±4.9	268±2.1	3.2±1.6	−	[104]
	CSIR Rheo-HPDC	T6	317±3.6	261±1.4	6.7±1.9	−	[104]
	CSIR Rheo-HPDC	AF	218±2.5	113±3.0	10.6±1.6	−	[104]
	CS Rheo-SC	AF	232	−	7	−	[105]
	SC	AF	208	−	6	−	[105]
	SIM Rheo-HPDC	AF	271	−	7.17	−	[39]
	HPDC	AF	211.5−220.8	−	5.4-6.7	−	[106]
	SCP Rheo-HPDC	AF	249.8−250.1	−	12.5-13.2	−	[106]
	SCP Rheo-HPDC	T6	327.8−331.2	−	9.8-11.3	−	[106]
	LSPSF Rheo-HPDC	T6	330	240	13	−	[34]
	RBRM Rheo-HPDC	AF	230	−	10.2	−	[107]
	HPDC	AF	210	−	6.8	−	[107]
	HPDC	AF	221±17	148±6	3.7±1.4	70±9	[63]
	DCC Rheo-HPDC	AF	266±7	175±5	8.8±0.7	78±7	[63]
7075	HPDC	AF	227.7−243.3	−	5.55	−	[46]
	ICSPC Rheo-HPDC	AF	293.1−299.5	−	1.65	−	[46]
	ICSPC Rheo-HPDC	T6	461.6−489.5	−	1.2	−	[46]
	CSIR Rheo-HPDC	T6	516	453	5.3	−	[108]
	Metal casting	T6	290−350	−	2-4	−	[109]
	CS Rheo-SC	AF	211−288	−	1.8-3	−	[109]
	CS Rheo-SC	T5	425	−	4.8	−	[109]
	CS Rheo-SC	T6	453	−	4	−	[109]
	CS Rheo-SC	T7	437	−	3.7	−	[109]
	CS Rheo-SC	T6	502	−	5.3	−	[109]
	HPDC	AF	281±25	222±9	1.6±0.9	86±14	[43]
	FCR Rheo-HPDC	AF	337±11	249±6	5.2±0.6	96±11	[43]
	FCR Rheo-HPDC	T6	543±15	506±9	4.1±0.7	172±15	[43]
	LSPSF Rheo-HPDC	AF	290-310	−	−	−	[36]
	LSPSF Rheo-HPDC	T6	483	−	8	−	[36]
	GISS Rheo-HPDC	T6	486	−	2	−	[110]
	SCP Rheo-HPDC	AF	210−260	−	0.2-1.7	−	[53]
	SCP Rheo-HPDC	T6	420−453	−	1.0-1.4	−	[53]
	HPDC	AF	293	231	1.8	−	[111]
	ACSR Rheo-HPDC	AF	351	254	3.9	−	[111]
	ACSR Rheo-HPDC	T6	547	494	3.2	−	[111]
	Forged	T6	572	503	11	−	[112]

HT: Heat treated; AF: As fabricated; HPDC: High pressure die casting; SC: Squeeze casting

Table 3 Tensile properties of AZ91 and AZ91D Mg alloys fabricated by different processes

Alloy	Process	HT	UTS/MPa	YS/MPa	EL/%	Hardness (HV)	Ref.
AZ91	HPDC	AF	186−212	−	3.2−5	−	[37]
	Rheo-HPDC	AF	215−227	−	4.8−6	−	[37]
AZ91D	HPDC	AF	212	146	3.3	−	[113]
	HPDC	AF	200	122	2.5	−	[114]
	Thixomolding	AF	240	−	4.5	−	[115]
	NRC	AF	230	−	5.5	−	[69]
	TBR Rheo-HPDC	AF	225	138	4.5	−	[116]
	RCP Rheo-HPDC	AF	255	157	2.3	−	[113]
	RDC	AF	248	145	7.4	−	[117]
	RDC	T4	230	91	11.2	−	[118]
	RDC	T5	236	133	6.5	−	[118]
	RDC	T6	255	134	6.7	−	[119]
	RDC	Tx	249	132	9.1	−	[119]
	FCS Rheo-HPDC	AF	265	169	7.1	−	[43]
	FCS Rheo-HPDC	T4	270	110	11.3	−	[43]
	FCS Rheo-HPDC	T6	282	171	5.8	−	[43]
	Rheomolding	AF	271	169	7.3	−	[120]
	HPDC	AF	205±12	142±7	2.8±0.6	73±9	[63]
	DCC Rheo-HPDC	AF	267±6	163±6	6,8±0.5	82±6	[63]

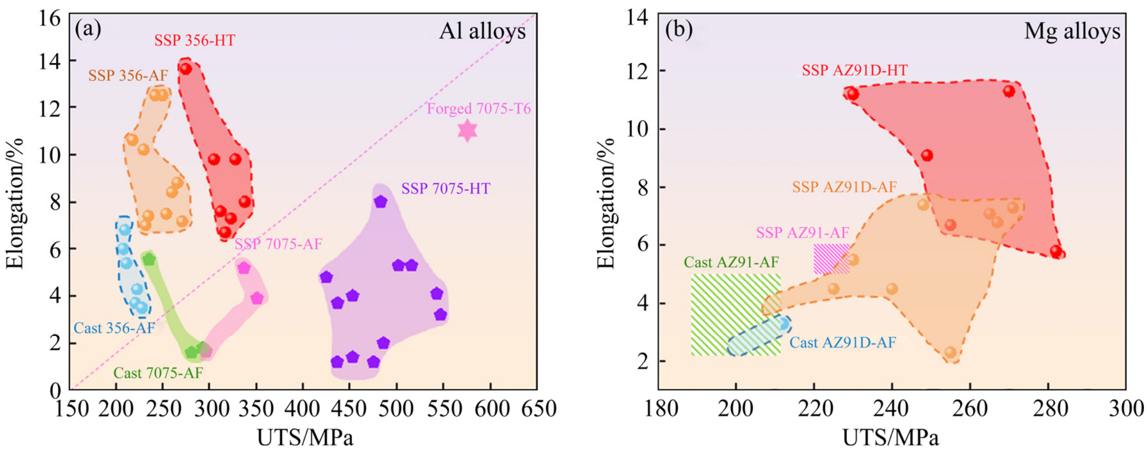

Fig. 5 Ultimate tensile strength versus elongation for some popular alloys processed by SSP and traditional processes in different conditions: (a) A356 and 7075 Al alloys; (b) AZ91 and AZ91D Mg alloys

has superior mechanical properties at elevated temperature than those of HPDC alloys because the refined and uniformly dispersed iron-rich intermetallic can prevent grain boundary sliding more effectively. Similar results have been also reported for hypereutectic Al−Si alloys.

3.2 Thermal conductivity

Researches on the thermal conductivity of SSP fabricated materials (normally Al alloys) are more recent. Al is an excellent conductor for electricity and thermal conductivity, coupled with its mass and price compared to copper (Cu), silver (Ag) and gold (Au) [10]. Therefore, Al alloys have attracted common attention and have been extensively studied for the last years, especially in the communication industry. It is widely accepted that the less porosity and higher relative density induced by SSP trigger preferable thermal conductivity. To date, a range of alloys with high thermal conductivity, such as Al8Si [72], Al7.5Si0.8Fe [59], Al−6Si−2Cu−Zn [121] alloys, that are suitable for SSP have been explored.

A comparison of thermal conductivity of some alloys is displayed in Fig. 6, demonstrating that SSP can effectively increase the thermal conductivity, posing an efficient strategy to remove excessive heat generated by the operation of devices. The thermal conductivity of these new alloys is higher than that of some common alloys like A383, A356, and A380 Al alloys. In addition, a series of Al alloys with an outstanding combination of heat, wear and thermal expansion properties have been developed for SSP by LIU et al [122], ZHONG et al [127] and XIONG [128]. It is known that as the Mg_2Si phase can expand the diffraction of electrons to reduce the average free path of electrons, 6063 Al alloy is a popular alloy that has medium strength with superb thermal conductivity. Nevertheless, systematic research on understanding the impact of SSP on the microstructure and performance of 6063 Al alloy is scarce.

4 Numerical modeling and simulation for SSP

As the process of SSP is not visible, numerical simulation technology has become one of the main methods to visualize it, explore its specific mechanism, and optimize the structure design of apparatus, and processing parameters in the slurry preparation and forming process. It is the other leg for the improvement of forming process compared with the experimental method. The modeling and simulation of the SSP have developed towards the integrated, multi-scale, and multi-physical-field direction.

Two important aspects in the numerical study are microstructure evolution and fluid flow together with their interactions. For the microstructure evolution, several methods are used, like stochastic methods Monte Carlo (MC) and Cellular Automata (CA), direct simulation methods phase field (PF), front tracking (FT) and level set (LS), and deterministic method. The most used methods are PF and CA. Because the PF method is based on the theory of free energy minimization of systems proposed by Ginzburg-Landau, the PF model becomes the preferred method in studying problems concerned with phase transformation. In the simulation about the rheological flow of semi-solid slurry, various apparent viscosity one-phase models and two-phase models have been developed, as summarized by ATKINSON [14]. The following section will be divided into two parts. One is for the overview of the microstructure evolution, while the other is for fluid flow.

4.1 Microstructure evolution

In studies about the microstructure evolution in semi-solid process, little effort has been made compared with other forming processes, like directional solidification, welding, and traditional casting. Although the foundation for the solidification is the same, the process parameters and typical eigenvalue about the thermodynamics

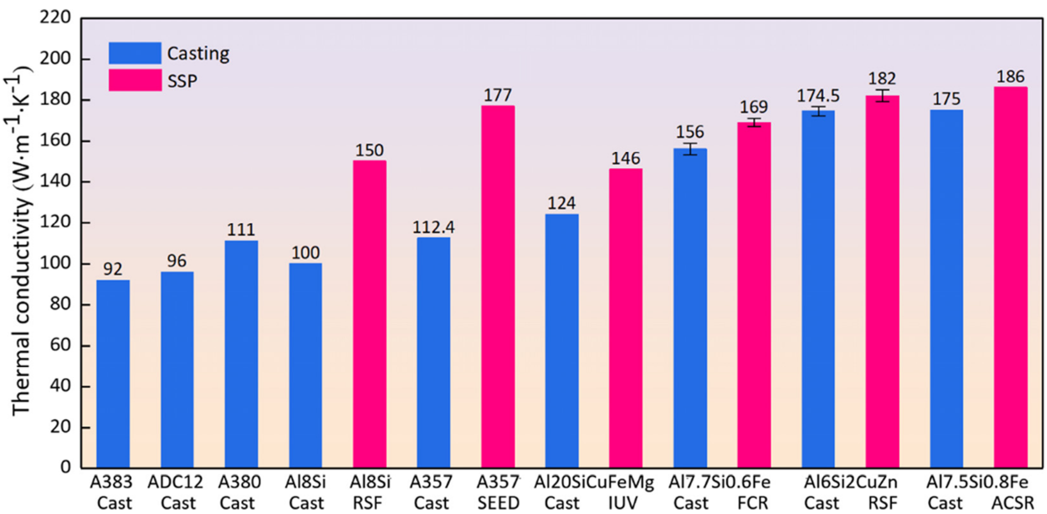

Fig. 6 Comparisons of thermal conductivities for SSP fabricated and some conventionally casting Al alloys [61,72,121−126]

and kinetics are different. Little difference in the eigenvalue may result in a different microstructure. To make the difference clear briefly, different process characteristic parameters are summarized and compared in Table 4. It can be seen from the data in Table 4 that only the effects of a single factor or a few variables on the microstructure morphology were studied, but the coupled influence has not been investigated sufficiently. The morphology of microstructure is the result of many factors, including the rate of temperature change, initial temperature, initial chemical composition, environmental pressure, holding temperature and time, temperature gradient, local melt convection degree, the addition of nucleating agent, and so on. Every phase transformation is driven by thermodynamic and kinetic variables. The experimental study focuses on the influence of macroscopic parameters on the final microstructure morphology. However, there are very complex interactions of microscopic parameters under macroscopic conditions. In-situ observation can obtain some microscopic details and reveal macroscopic phenomena to a certain extent. However, there is no quantitatively analyzable model, which can describe the relationship between field variables [142−146].

The information about the final microstructure, such as (1) intuitive understanding of various phase morphologies, (2) statistic data about the grain size, morphology, and volume fraction, (3) local solute distribution, and (4) transient information from in-situ experiments, can be obtained from the experimental study [66,147]. These data are almost final values or transient ones from interrupted experiments rather than continuous process ones, so the inner mechanism can only be deduced by inverted deriving a formula or verifying an existing theory. By contrast, it is a forward evolutionary process with full information about each variable field by numerical modeling while the simulation results can be verified by the experimental results. Numerical modeling and simulation are one powerful method to uncover the mechanism underneath the microstructure formation during the semi-solid process. However, the concentration

Table 4 Eigenvalue about thermal and kinetic data in different processes

Process	Alloy	Cooling rate/ ($°C\cdot s^{-1}$)	Undercooling degree/ °C	Temperature gradient/ ($°C\cdot mm^{-1}$)	Forced convection/ ($m\cdot s^{-1}$)	Perturbation
Semi-solid	Al−4.5%Cu [129]	−	20−40	−	0−0.1	−
Semi-solid	Al−2.0%Si [130]	−	−	−	−	0−0.4
Semi-solid	357.0 [131,132]	0.0162, 0.162, 1.62	2.5, 8.3, 16.3	0.230, 0.442, 0.657	0−0.735	0.0005
Cooling slope	A380 [133]	8.3−11	−	−	−	−
−	AZ91D [134]	1−2	−	−	0.055−0.22	−
Free solidification	Al−Pb, Al−Bi, Al−In, Cu−Pb [135]	−	−	0.6−1.0	−	−
Directional solidification	−	−	−	5.0−6.0	−	−
Fast solidification	Al−1Si, Al−3Si, Al−6Si, Al−9Si, Al−12Si, Al−15Si [136]	−	−	1.0×10^4	−	−
Directional solidification	SCN−ACE [137]	−	−	7	−	−
Directional solidification	Al−15Cu [138]	−	−	11	−	−
Ultrasonic	Bi−8%Zn [139]	−	−	5.2−6.4	−	−
Directional solidification	Al−Zn [140]	−	−	10.0−20.0	−	−
Welding	Cu/Sn−9Zn/Cu[141]	−	−	50.8	−	−

paid on this aspect is far from enough, especially in semi-solid processing. The status, problem, and possible directions of effort about the modeling and simulation for microstructure evolution in semi-solid forming will be analyzed and discussed below.

Although the existing numerical studies can depict some typical phenomena found in practice, (see Fig. 7) a universally accepted explanation for the mechanism has not been found. Table 5 shows that the numerical work concerned grain growth in the semi-solid slurry is very limited. Since there is no systematic and perfect parameter and simulation system, it is not portable to simulate the microstructure of different alloys with different process parameters. Variation of process parameters will affect some phase transition coefficients (like solute partition coefficient, solidus, and liquidus, etc.) in a certain way. But how and to what extent these coefficients have been affected have not been studied. The existing simulation work only uses empirical values, which are not properly modified when applied to alloys with different compositions. At present, high-performance computing and model optimization have made great progress. The computing power and model convergence stability have been greatly improved. Then much fundamental research needs to be done about the material properties and solidification characteristics to improve simulation accuracy.

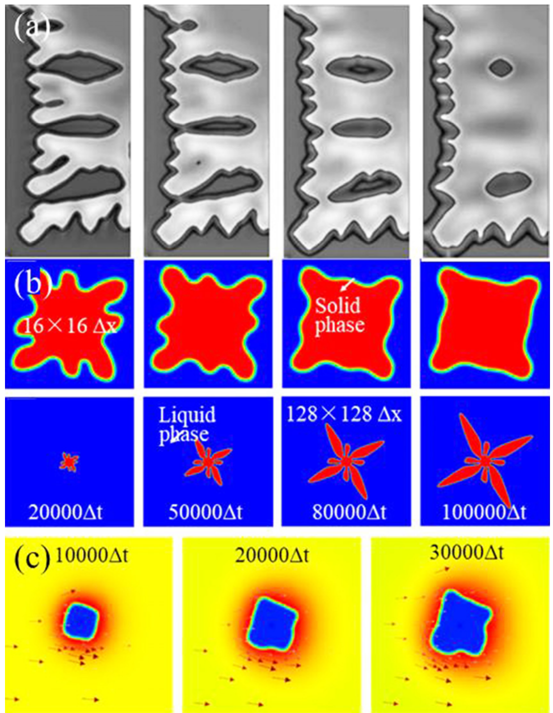

Fig. 7 Typical phenomena depicted in numerical simulation: (a) Detaching [148]; (b) Nucleation effect [131]; (c) Fluid flow effect [131]

4.2 Fluid flow simulation

The flow simulation of the mold filling process is another one of the most interesting aspects. Although many models concerned with one-phase or multiphase and simulation methods have been proposed, as summarized in Ref. [14], these models and simulation methods are not universal, but only applicable to a certain alloy, product, and process. The reason is because of the multiple properties of semi-solid slurry. Its macroscopic flow conforms to the power-law model of shear thinning, while the microscopic movement of its internal particles conforms to the multiphase flow theory. Three

Table 5 Status about microstructure simulation in semi-solid process

Method	Alloy	Static anisotropy coefficient	Kinematic anisotropy coefficient	Liquid/solid surface energy/ ($J\cdot cm^{-2}$)	Kinetic coefficient between phases/ ($cm^4\cdot J^{-1}\cdot s^{-1}$)	Gibbs−Thomson coefficient/ (m·K)	Lewis number
PF	A380 [133]	0.5	0.2	2×10^{-5}	0.05	–	–
PF	Binary alloy [148]	–	–	–	–	–	–
PF	357.0 [131]	0.02	–	–	–	–	1
PF	357.0 [132]	0.02	–	–	–	–	1
PF	357.0 [149]	0.02	–	–	–	–	1
CA	A356 [150]	–	–	–	–	9×10^{-8}	–
CAFÉ	Al−7Si [151]	–	–	–	–	2×10^{-7}	–
Self-developed software	AZ91D [134]	–	–	–	–	–	–

viewpoints about the multiphase nature of semi-solid slurry are drawn from the literatures and listed in Table 6. These viewpoints artificially divide the two phases in the slurry, and there is a certain deviation between the established model and the reality. Liquid and solid particles in the semi-solid slurry are an organic whole, and they interact with each other in complex ways. However, the current studies only focus on the macroscopic rheological flow behavior or the internal multiphase flow characteristics, and do not combine the two organically to study the constitutive flow behavior. Figure 8 shows the efforts and simulation results of establishing a two-phase flow model by considering interphase interactions [156,157]. Although the spatial distribution of the solid phase can be depicted and has a certain accuracy compared with the experimental results, it is difficult to visualize the granular phase as separate particles.

The next research direction is combining CFD and DEM, and coupling the microstructure characteristics with the macroscopic rheological properties to establish a rheological model of slurry based on its internal microstructure characteristics. This model is not the one that only takes a slurry temperature or solid fraction as variables but considers the size, morphology, and volume fraction of the solid particles in the slurry as essential variables. The corresponding numerical results will give more details about the forming process of phase segregation, porosity, and other filling defects, also the final microstructure which determines the performance of products. This detailed information is critical to process optimization.

5 Industrial application

5.1 General situation

SSP of Al and Mg alloys has been investigated and developed for about half a century. In 1978, Alumax engineered metal process (AEMP, USA) has established an SSP production line, which means that SSP technology has entered the stage of industrial application research. Since then, more production lines have been set up in Europe, the United States and so forth. Since the 1980’s, China has been involved in SSP research, which has gradually attracted the extensive attention of scholars. In 2000, researchers from mainland China first participated in the 6th International Conference

Table 6 Three viewpoints about multiphase property of semi-solid slurry

Semi-solid slurry	Point 1 [152]	Point 2 [153]	Point 3 [154]
Solid phase	Skeleton	Non-Newtonian	Viscoplastic+yield
Liquid phase	Darcy’s law	Newtonian	Newtonian

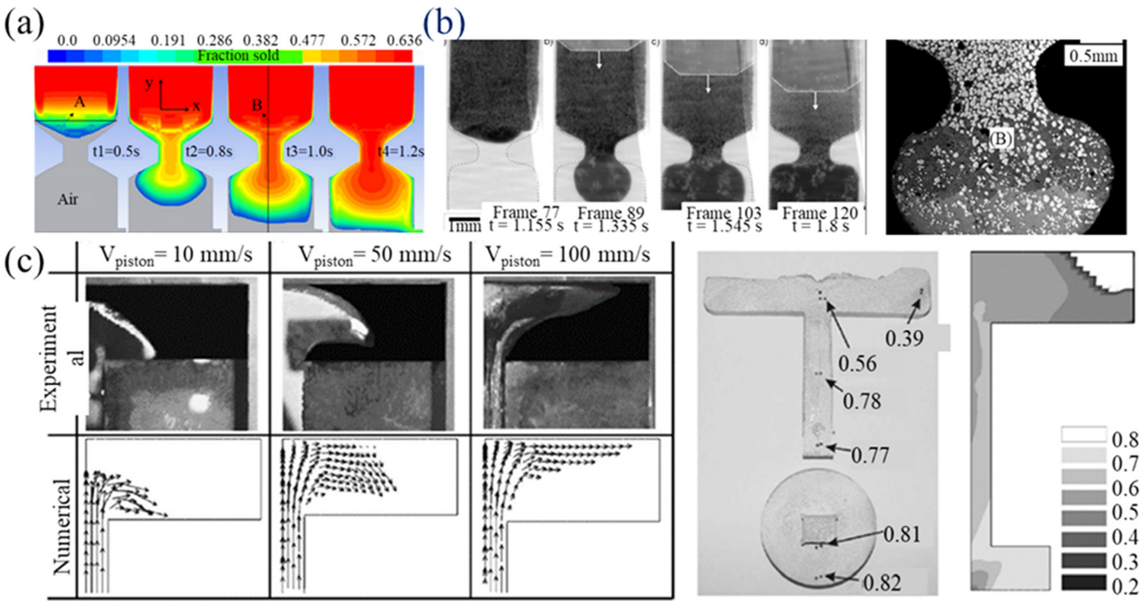

Fig. 8 Simulation of fluid flow during SSP: (a) Two-phase simulation [155]; (b) In-situ observation [156]; (c) Two-phase flow, and experiment results of T-shape cavity [157]

on SSP held in Italy, and the studies on SSP technology were rising. Furthermore, the SSP technology was officially listed in the "industrial development catalog in China" in 2011, marking the application in China's industrialization. Since 2010, the upsurge of research and application of SSP in the world seemed to fade. But there seems to be a resurgence in demand for SSP as demonstrated by a considerable number of participants at the 15th SSP Conference in Shenzhen, China (S2P 2018) [21].

Although the research of SSP in China is relatively late, great progress has been achieved with the support of a collection of policies and funds and with the drive of industrial upgrading. Recently, as a huge industrial power and potential market, China immensely promotes the application of SSP primarily due to the automobile lightweight and the upgrading of communication equipment. Currently, at least 30 enterprises focus on the research and development (R&D) of SSP in China, whereas the number for North America and Europe is relatively limited. Similar to the distribution pattern of other manufacturing industries in China, the SSP enterprises are mostly situated in the eastern coastal areas, particularly in the Pearl River Delta (PRD) and Yangtze River Delta (YRD) regions. It also should be noted that the COVID-19 has been basically well controlled in China, which is also favorable in the recovery and development of the SSP industry.

As discussed in Section 2.1, only very limited number of SSP technologies are suitable for large-scale practical production and commercial development. For Mg alloys, thixomoulding is the dominant process in the world [1]. The major SSP of Al alloys applied in China is rheocasting in terms of SEED, RSF/RheoMetal and GISS processes, and they have a wide range of applications, as listed in Table 7. Very recently, the DCC and ACSR processes are also gaining favor quickly across the academic and industrial sectors [28,60]. Some recent examples of successful development and applications in China will be

Table 7 SSP processed products in production [158]

Application field	GISS	RSF/RheoMetal	SEED
Automotive	Auto gearbox	Compressor parts	Brackets
	Brake system components	Cooling units for power electronics	Control arm
	Chain covers		Engine bearing cap
	Engine block		Engine bracket
	Oil pan		Shock towers
	Steering wheels		Turbo impeller
Electronics	Handphone covers	Heat sinks	Heat sinks
	Hard disc drive housing	Radio filters 4G and 5G	Radiator housing
	Heat sinks		
	Radio filters 4G and 5G		
Heavy duty truck components	Truck gearbox	Muffler holders	Brake calliper
			Brackets
			Knuckle
			Skeleton joint
Machinery		Machine parts with steel inserts	
Marine application	Sacrificial anode	Winch housing	
Medical components	Prosthetics		
Military components	Cast 7075 composite armour plate		
Sports	Bicycle components	Bicycle components	Motocross frame
	Motorcycle parts		Wheel knuckle

exhibited and discussed in more detail in the next section.

5.2 Some outstanding cases

As illustrated in Figs. 9(a−d), a sequence of Al components has been redesigned for automotive by our team. These Al components have replaced conventional steel parts and a significant mass reduction of 35%−65% was achieved. Figure 9(e) demonstrates the performance comparison of radiator housing processed by SEED Rheo-HPDC and traditional HPDC, signifying that the SEED process can markedly improve the thermal conductivity while noticeably reducing the cost and mass. This promising method was also used to explore and manufacture a series of Al parts in various sectors, such as steering knuckle for passenger cars, bracket for commercial vehicles, inverter main box for new energy vehicles and communication cavity used in communication industry, as shown in Fig. 10. As illustrated in Figs. 9 and 10, the outline of the parts fabricated by SEED process is quite clear without obvious defects and exhibit high surface quality, illustrating that the mold filling process is quite satisfactory.

The RSF process, introduced into China in 2008, with over 30 machines delivered, has mainly found its applications within light emitting diode (LED) fittings and heat sinks, as well as other applications within the transportation industries, as shown in Figs. 11(a−h). Some application examples from marine equipment, sports equipment and

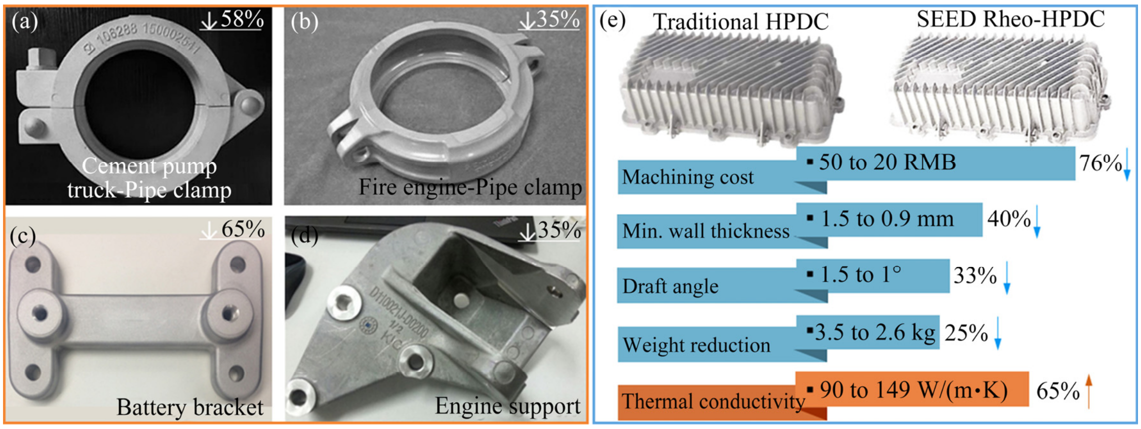

Fig. 9 Al parts fabricated by SEED: (a) Pipe clamp for cement pump truck; (b) Pipe clamp for fire engine; (c) Battery bracket; (d) Engine support; (e) Radiator housing

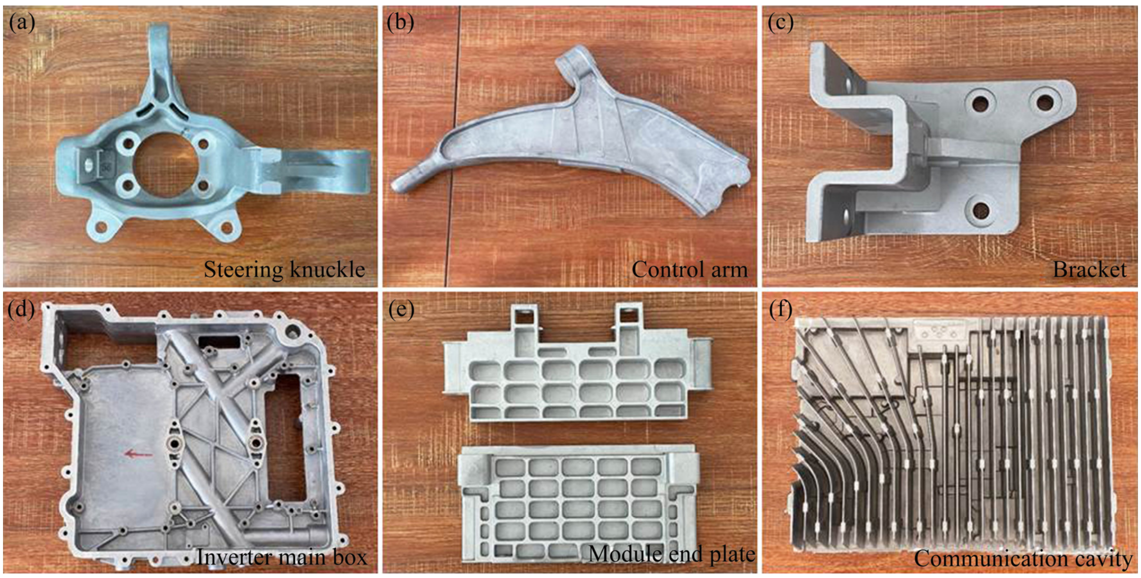

Fig. 10 Some SEED produced components used in various sectors: (a) Steering knuckle; (b) Control arm; (c) Bracket; (d) Inverter main box; (e) Module end plate, (f) Communication cavity

railway transport have also been illustrated. For example, the lock body (Fig. 11(d)), one of the key components of high-speed train door produced by the CAM (Jiangle) Institute of Semi-solid Metal Technology (Sanming, China), has brought about a mass reduction of 65% with machining reduction by half. The V-shaped radiating tooth filter housing, as shown in Fig. 11(i), with middle disconnection and with minimum tooth thickness of 1.1 mm displays the clearly discernible outlines and excellent surface quality of the shell part, signifying that the mold filling is well-pleasing.

Figure 12 shows some typical automobile and communication products fabricated by ACSR Rheo-HPDC. These parts were developed by the group in the University of Science and Technology

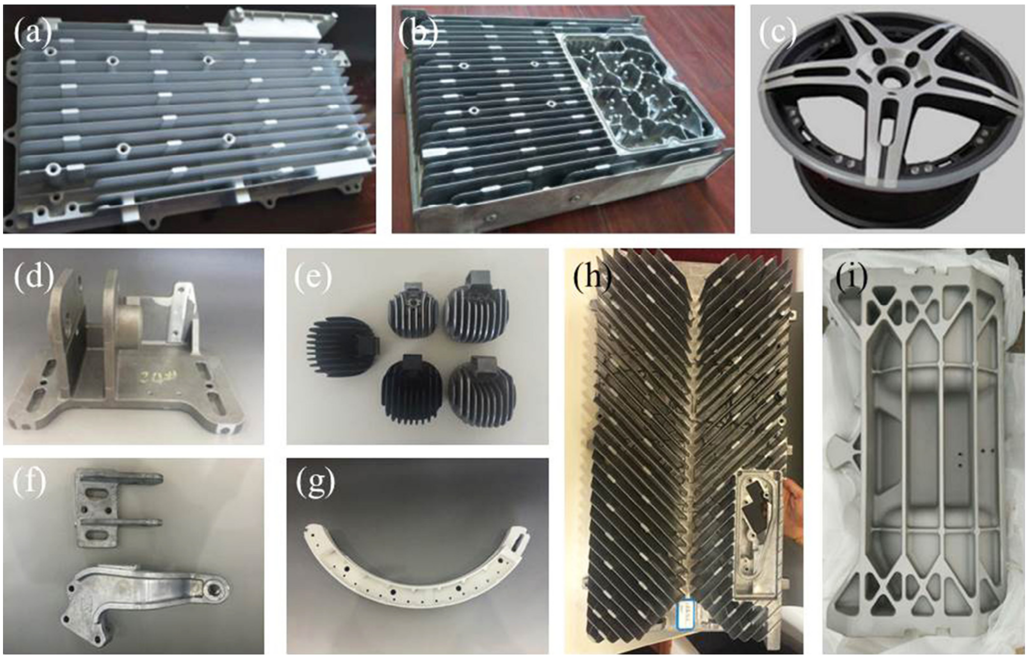

Fig. 11 RSF fabricated components: (a, b) Al−8Si telecommunication parts with complex structure; (c) Auto-hub; (d) Lock body; (e) LED fittings; (f) Swing arm; (g) Explosion-proof tire bracket; (h) V-shaped radiating tooth filter housing; (i) Crossbeam for new energy vehicles [72,159]

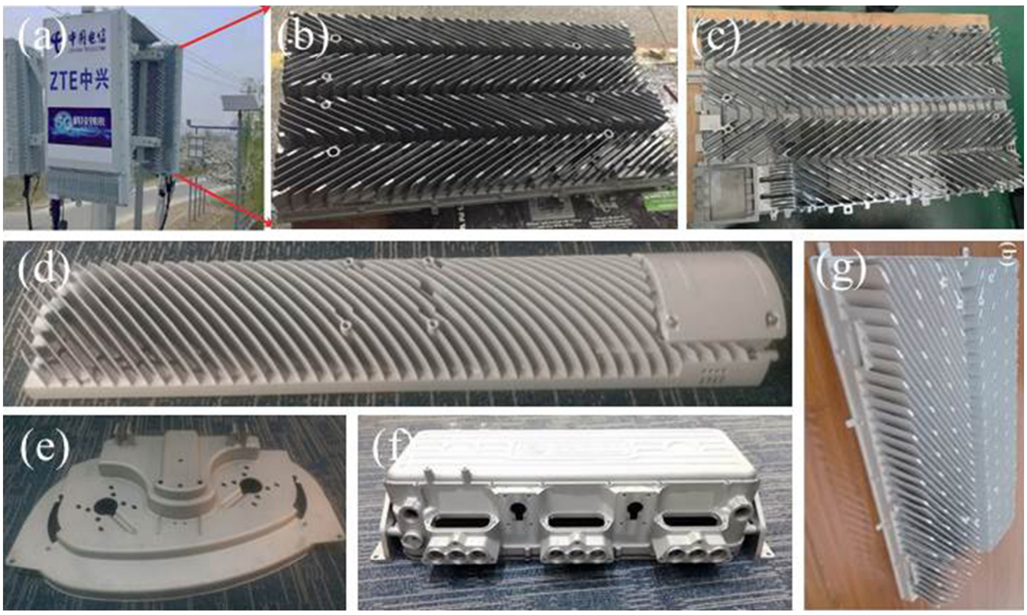

Fig. 12 Typical ACSR Rheo-HPDC products: (a−c) Application scenario and morphology of large thin-walled 5G base station heat dissipation shells; (d) 4G heat dissipation shells; (e) New energy vehicle end cover; (f) New energy vehicle power converter shell; (g) Another large thin-walled 5G base station heat dissipation shells [61,160]

Beijing (Beijing, China) and were produced by Zhuhai Runxingtai Electric Appliance Co., Ltd (Zhuhai, China). Dozens of production lines have been built at Zhuhai and over 3 million components are manufactured each year [21]. Figures 12(a−c) display the application scenario, the front and the back of large thin-walled 5G communication base station heat dissipation shells, with outer dimensions of 933 mm × 470 mm × 80 mm, a tooth thickness of 1 mm, and a tooth height of 70 mm [61]. A recent large thin-walled part is also exhibited in Fig. 12(g), with the external dimensions of 878 mm × 447 mm × 171 mm [160]. These successful applications have proved again the feasibility of SSP to grapple with the issue of large thickness difference of the thin-walled parts, which has long been regarded as a thorny problem in the casting industry. Furthermore, these ACSR fabricated components for different applications also demonstrate higher strength and elongation, higher heat conductivity, more excellent corrosion resistance and mass reductions in comparison with traditional casting [59].

The GISS process has found the broadest range of applications, and over 70 companies are using this powerful technology in China for the mass-production of automotive parts and communication components [20,63,158,161]. It is recently reported that GISS has been commercially used in almost all areas, but the dominant field is within the communication and electronics industry [158]. The improved productivity and reliability, low cost, and good comprehensive performance of components are the main elements for them to win the favor of the market [20,161]. As displayed in Fig. 13, it is feasible for GISS to precisely produce the communication components that always have multifarious characteristics and sizes.

6 Summary and outlook

6.1 Summary

The past several years have witnessed the significant progress of the SSP in the fundamental research and industrial applications in China. In this review, we first focus on discussing the development of slurry preparation methods and recent innovations of the SEED process. Subsequently, the performance of components fabricated by SSP in terms of tensible behavior and thermal conductivity are overviewed. Then the foundation understanding about the microstructure evolution and rheological flow behavior obtained by numerical modeling and simulation is reviewed and discussed. Finally, we summarize the current general situation of industrial application and present a range of successful examples. The remarkable success has definitely established SSP among the competitive approaches for fabricating high-quality components due to its low cost, short process and low energy consumption. SSP will contribute to the further development and exploration of processing cost-effective and complex structural components in a range of industries in the future.

6.2 Outlook

With the rapid pace of industrialization, industrial parts made in China occupy more and more share in the international market [162−164]. At present, China is the large automobile consumer market in the world, and the annual sales of the sixth straight year have been more than 24 million, as shown in Fig. 14(a). In addition, although the outbreak and spread of COVID-19 shatter the global automotive industry, China has not been greatly affected and constitutes over 32.4% of the

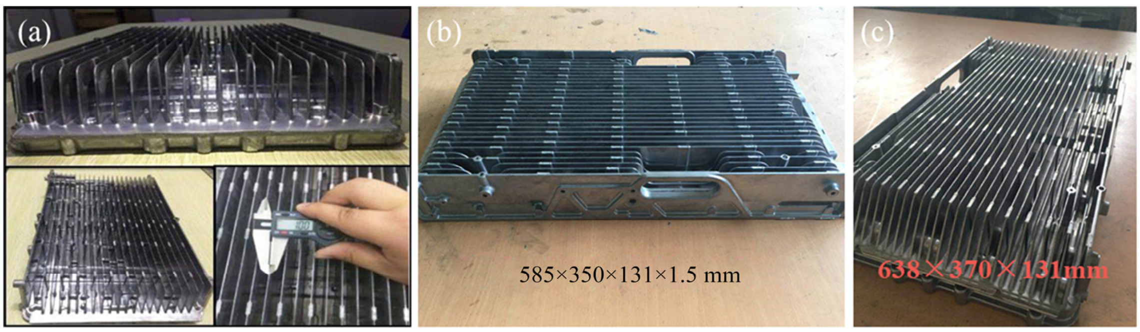

Fig. 13 Application cases of communication parts with various shapes and sizes processed by GISS

world's car sales in 2020, hitting record levels. There was also a dramatic increase in the number of base stations in China, as shown in Fig. 14(b). It is reported that China has built the world's largest communication network, with 5.75 million 4G and 0.72 million 5G base stations, accounting for more than 50% and 70% of the world's total, respectively. Following the swift growth of automotive and communication industries, high-quality components with low cost are eagerly desired, which brings a promising opportunity for the development and application of SSP of Al and Mg alloys [5,167].

Overview of SSP of Al and Mg alloys regarding some key aspects and characteristics is displayed in Fig. 15, indicating that there is quite a long process from scientific spark to engineering realization. Based on the previous studies, this section primarily summarizes the current deficiencies of SSP of Al and Mg alloys in both scientific and application sectors, and presents an outlook for the follow-up research work and delivers guidelines on the future progress of this frontier field.

(1) It is widely known that materials should be designed for their processing route. But, so far, almost all the materials that are widely used in SSP are developed for traditional processes, as shown in Table 1. Hence, effective control during the slurry

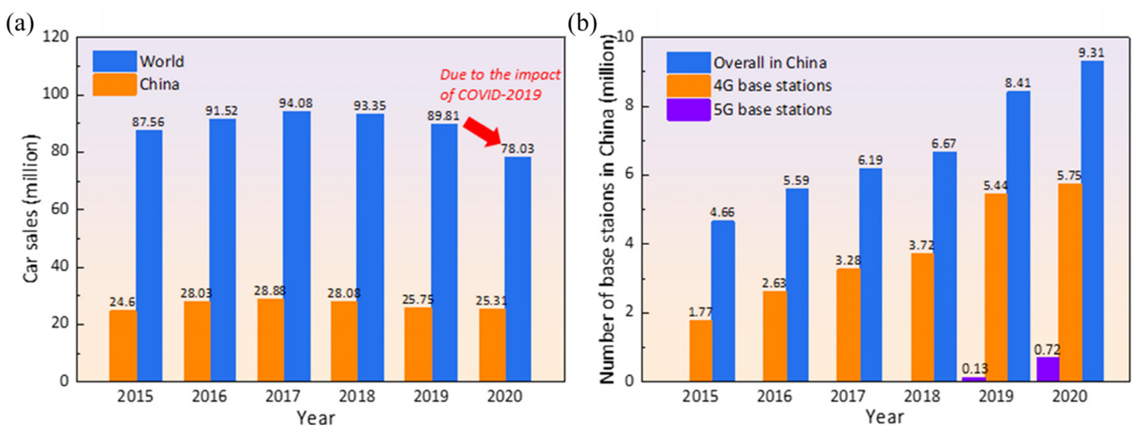

Fig. 14 Statistical data of number of annual car sales in China and world (a) [165] and built base stations over past six years (b) [166]

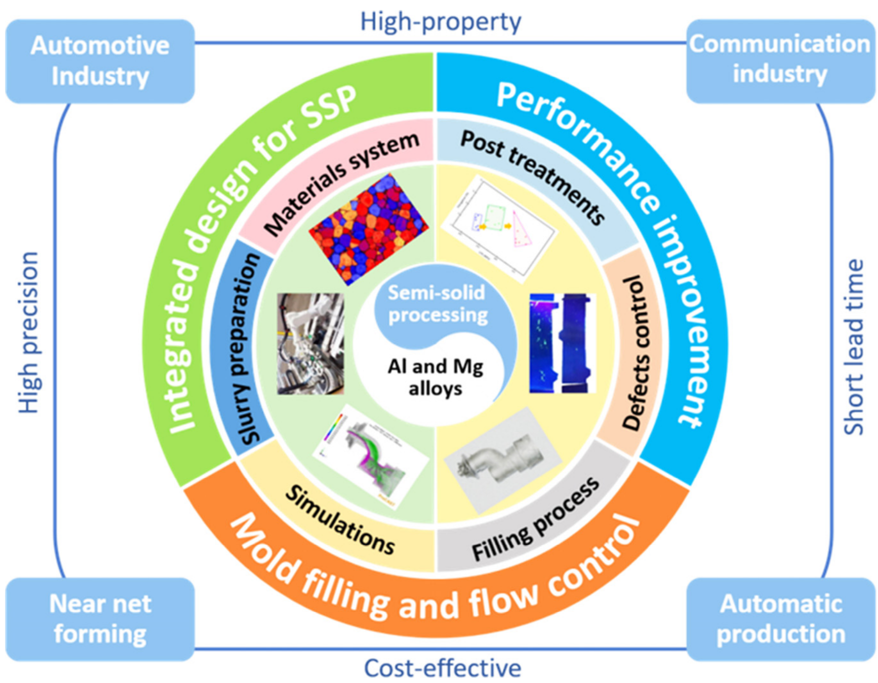

Fig. 15 Overview of SSP of Al and Mg alloys with regard to technique route, basic steps, advantages and application fields

preparation is lacking. The complete and in-depth understanding of the structure-property relationship is necessary to improve the performance of the products. Accordingly, besides the advances regarding the readily-available alloys, developing or tailoring more reliable alloys specifically for SSP that consider both the process needs and the target properties concurrently is significantly crucial [5,18]. For instance, various requirements are proposed for the automotive components, e.g., high strength, high fatigue resistance, creep resistance or wear resistance. Even though some materials have been successfully developed, different material systems are highly desired to fulfill more requirements for industrial applications [168,169].

(2) As aforementioned, only a small part of SSP methods can successfully achieve industrial production. Thus, it is of vital importance to optimize existing methods or develop novel methods that can have both improved production efficiency and good stability during slurry preparation and subsequent processing. Moreover, the performance of SSP fabricated parts is hard to reach the same level as the forged counterparts. This is also an important reason why SSP is hard to have a huge market share. Accordingly, it is also essential to further understand and control the defects formed in SSP fabricated parts, such as blowholes, blisters and hot cracks to improve the comprehensive performance [170−174]. In addition, SSP is now mainly adopted in the transportation and communication communities, so this competitive technology is expected to explore its applications in more fields, like the aerospace field and wearable devices.

(3) As the process of SSP is not visible, numerical simulation technology has become one of the main methods to visualize it, explore its specific mechanism, and optimize the structure design of apparatus and process parameters in the slurry preparation and forming process. The flow simulation of the mold filling process is one of the most interesting aspects. Although many models concerned with one-phase [15] or multiphase [155] and simulation methods have been proposed, these models and simulation methods are not universal, and only applicable to a certain alloy, product, and process. The reason is because of the multiple properties of semi-solid slurry. Its macroscopic flow conforms to the power-law model of shear thinning, while the microscopic movement of its internal particles conforms to the multiphase flow theory. However, the current studies only focus on the macroscopic non-Newtonian flow behavior or the internal multiphase flow characteristics, and do not combine the two organically to study the constitutive flow behavior. The solution is to couple the microstructure characteristics with the macroscopic rheological properties and establish a rheological model of slurry based on its internal microstructure characteristics, which is not the one that only takes a slurry temperature or solid fraction as variables.

(4) Along with the development of the global economy, the market is extremely exacting on price and lead time, which requires the supply chain to foster and promote the core competence. With the rapid development of the artificial intelligence (AI), the highly integrated design and intelligent control of the SSP equipment are highly needed to ulteriorly improve the production efficiency and reduce the cost. For example, special dies and molds for SSP have been developed to improve the mechanical properties and reduce the cost [175−178]. It should also be noted that although SSP can provide considerable cost-saving, high performance, and high structural complexity of parts, there is a relatively long procedure to develop qualified parts and hence many technical problems will inevitably arise, as shown in Fig. 16. That requires concerted efforts and working hand in glove between demand-side and alloy/process developers to develop and produce new parts and promote the SSP to a commercially acceptable level. In addition, it is also essential for universities and institutions to provide talent support and knowledge contribution for SSP development by cultivating motivated and excellent students and highly skilled technicians.

(5) Although SSP has been developed for almost half a century, the systematic industry specification or standard for SSP is still scarce, which is not beneficial to the further promotion and development of SSP. Fortunately, some enterprises in China have developed their own internal standards, such as Dongfeng Motor, Beijing Foton Daimler Automotive and Shaanxi Heavy Duty Automobile Co., Ltd. In addition, a national specification on process called “Casting aluminum

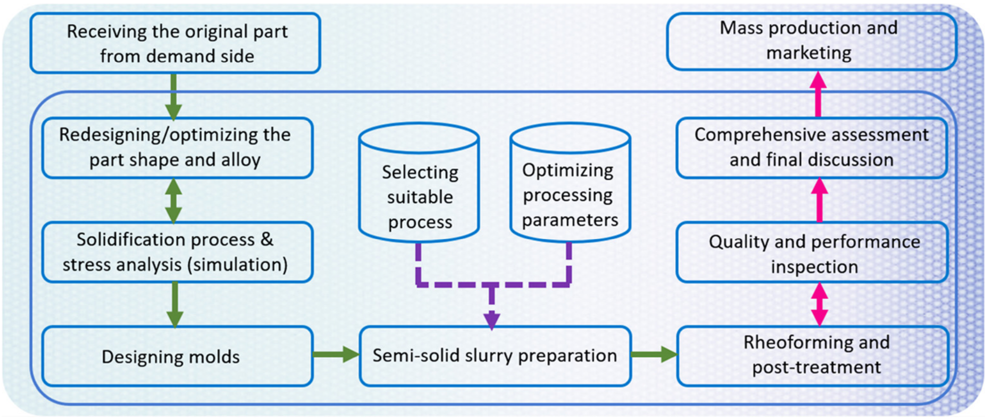

Fig. 16 Flow diagram of developing new parts suitable for SSP

alloys—Process specification for semisolid rheo-diecasting forming (GB/T 40809—2021)" has been released and will be officially implemented in May 2022.

As a concluding remark, it has been proven that SSP is a powerful approach in the mass-production of high-performance components with some successful cases in China. Significantly, the SSP fabricated parts have demonstrated excellent properties that basically meet the demand of markets. Meanwhile, their fabrication is readily scalable and cost-effective, which provides a solid function for industrial production. Therefore, we propose that SSP will shed light on the landscape of batch fabrication for the next generation of advanced structural components and contribute to the realization of "Made in China 2025".

Acknowledgments

The authors are grateful for the financial supports from the Shenzhen Science and Technology Innovation Commission, China (Nos. KQTD20170328154443162, JCYJ20180305123432756).

References

[1] CZERWINSKI F. Semisolid processing of magnesium alloys: Progress and limitations [J]. Solid State Phenomena, 2019, 285: 489−494.

[2] SUN W W, ZHU Y M, MARCEAU R, WANG L Y, ZHANG Q, GAO X, HUTCHINSON C. Precipitation strengthening of aluminum alloys by room-temperature cyclic plasticity [J]. Science, 2019, 363(6430): 972−975.

[3] MO N, TAN Q Y, BERMINGHAM M, HUANG Y D, DIERINGA H, HORT N, ZHANG M X. Current development of creep-resistant magnesium cast alloys: A review [J]. Materials & Design, 2018, 155: 422−442.

[4] WILLIAMS J C, STARKE E A Jr. Progress in structural materials for aerospace systems [J]. Acta Materialia, 2003, 51(19): 5775−5799.

[5] LI G, LU H X, HU X G, LIN F, LI X W, ZHU Q. Current progress in rheoforming of wrought aluminum alloys: A review [J]. Metals, 2020, 10(2): 238.

[6] ZHU Q, MIDSON S P. Semi-solid moulding: Competition to cast and machine from forging in making automotive complex components [J]. Transactions of Nonferrous Metals Society of China, 2010, 20(S3): s1042−s1047.

[7] GUO C, XU Z, ZHOU Y, SHI S, LI G, LU H X, ZHU Q, WARD R M. Single-track investigation of IN738LC superalloy fabricated by laser powder bed fusion: Track morphology, bead characteristics and part quality [J]. Journal of Materials Processing Technology, 2021, 290: 117000.

[8] LI G, GUO C, GUO W F, LU H X, WEN L J, HU X G, ZHU Q. Influence of selective laser melting process parameters on densification behavior, surface quality and hardness of 18Ni300 steel [J]. Key Engineering Materials, 2020, 861: 77−82.

[9] LI G, LI X W, GUO C, ZHOU Y, TAN Q Y, QU W Y, LI X G, HU X G, ZHANG M X, ZHU Q. Investigation into the effect of energy density on densification, surface roughness and loss of alloying elements of 7075 aluminium alloy processed by laser powder bed fusion [J]. Optics & Laser Technology, 2022, 147: 107621.

[10] ABOULKHAIR N T, SIMONELLI M, PARRY L, ASHCROFT I, TUCK C, HAGUE R. 3D printing of aluminium alloys: Additive manufacturing of aluminium alloys using selective laser melting [J]. Progress in Materials Science, 2019, 106: 100578.

[11] WANG Pei, ECKERT J, PRASHANTH K G, WU Ming-wei, KABAN I, XI Li-xia, SCUDINO S. A review of particulate-reinforced aluminum matrix composites fabricated by selective laser melting [J]. Transactions of Nonferrous Metals Society of China, 2020, 30(8): 2001−2034.

[12] TAN Q Y, ZHANG J Q, SUN Q, FAN Z Q, LI G, YIN Y, LIU Y G, ZHANG M X. Inoculation treatment of an additively manufactured 2024 aluminium alloy with titanium nanoparticles [J]. Acta Materialia, 2020, 196: 1−16.

[13] ATKINSON H V, FAVIER V. Does shear thickening occur in semisolid metals? [J]. Metallurgical and Materials Transactions A, 2016, 47(4): 1740−1750.

[14] ATKINSON H V. Modelling the semisolid processing of metallic alloys [J]. Progress in Materials Science, 2005, 50(3): 341−412.

[15] HU X G, ZHU Q, ATKINSON H V, LU H X, ZHANG F, DONG H B, KANG Y L. A time-dependent power law viscosity model and its application in modelling semi-solid die casting of 319s alloy [J]. Acta Materialia, 2017, 124: 410−420.

[16] ATKINSON H. Current status of semi-solid processing of metallic materials [J]. Advances in Material Forming, 2007: 81−98.

[17] MODIGELL M, POLA A, TOCCI M. Rheological characterization of semi-solid metals: A review [J]. Metals, 2018, 8(4): 245.

[18] ROGAL Ł. Critical assessment: Opportunities in developing semi-solid processing: Aluminium, magnesium, and high-temperature alloys [J]. Materials Science and Technology, 2017, 33(7): 759−764.

[19] ZHU Q, MIDSON S, MING C W, ATKINSON H V. Casting and heat treatment of turbocharger impellers thixocast from alloy 201 [J]. Solid State Phenomena, 2012, 192/193: 556−561.

[20] WANNASIN J, FUCHS M, LEE J Y, LEE C U, NARASIMHA RAO T V L, FLEMINGS M C. GISS technology: Principle and applications in die casting [J]. Solid State Phenomena, 2019, 285: 470−475.

[21] KAPRANOS P. Current state of semi-solid net-shape die casting [J]. Metals, 2019, 9(12): 1301.

[22] LI D Q, ZHANG F, MIDSON S P, LIANG X K, YAO H. Recent developments of rheo-diecast components for transportation markets [J]. Solid State Phenomena, 2019, 285: 417−422.

[23] LI G, LU H X, HU X G, ZHU Q. Numerical simulation of slurry making process of 7075 aluminum alloy under electromagnetic field in rheocasting process [J]. Solid State Phenomena, 2019, 285: 373−379.

[24] WANNASIN J, MARTINEZ R A, FLEMINGS M C. Grain refinement of an aluminum alloy by introducing gas bubbles during solidification [J]. Scripta Materialia, 2006, 55(2): 115−118.

[25] LIANG X K, ZHU Q, LUO M, LI D Q. Application of polarized light microscopy on microstructural characterization of semisolid slurry [J]. Rare Metals, 2018: 1−8.

[26] WU S S, XIE L Z, ZHAO J W, NAKAE H. Formation of non-dendritic microstructure of semi-solid aluminum alloy under vibration [J]. Scripta Materialia, 2008, 58(7): 556−559.

[27] JANUDOM S, WANNASIN J, BASEM J, WISUTMETHANGOON S. Characterization of flow behavior of semi-solid slurries containing low solid fractions in high-pressure die casting [J]. Acta Materialia, 2013, 61(16): 6267−6275.

[28] QI M F, KANG Y L, QIU Q Q. Industrialized application of Rheo-HPDC process for the production of large thin-walled aluminum alloy parts [J]. Solid State Phenomena, 2019, 285: 453−458.

[29] CZERWINSKI F. Thermomechanical processing of metal feedstock for semisolid forming: A review [J]. Metallurgical and Materials Transactions B, 2018, 49(6): 3220−3257.

[30] WU S S, LÜ S, AN P, NAKAE H. Microstructure and property of rheocasting aluminum-alloy made with indirect ultrasonic vibration process [J]. Materials Letters, 2012, 73: 150−153.

[31] LÜ S, WU S S, LIN C, HU Z Q, AN P. Preparation and rheocasting of semisolid slurry of 5083 Al alloy with indirect ultrasonic vibration process [J]. Materials Science and Engineering A, 2011, 528(29/30): 8635−8640.

[32] LÜ S, XIAO P, YUAN D, HU K, WU S. Preparation of Al matrix nanocomposites by diluting the composite granules containing nano-SiCp under ultrasonic vibaration [J]. Journal of Materials Science & Technology, 2018, 34(9): 1609−1617.

[33] LÜ S, WU S S, YANG X, HAO L Y, GUO W, FANG X G. Microstructure and mechanical properties of $Mg_{97}Zn_1Y_2$ alloy reinforced with LPSO structure produced by semisolid squeeze casting [J]. Materials Science and Engineering A, 2018, 732: 359−367.

[34] GUO H M, YANG X J, WANG J X. Pressurized solidification of semi-solid aluminum die casting alloy A356 [J]. Journal of Alloys and Compounds, 2009, 485(1/2): 812−816.

[35] GUO Hong-min, YANG Xiang-jie. Preparation of semi-solid slurry containing fine and globular particles for wrought aluminum alloy 2024 [J]. Transactions of Nonferrous Metals Society of China, 2007, 17(4): 799−804.

[36] GUO Hong-min, YANG Xiang-jie, WANG Jia-xuan, HU Bin, ZHU Guang-lei. Effects of rheoforming on microstructures and mechanical properties of 7075 wrought aluminum alloy [J]. Transactions of Nonferrous Metals Society of China, 2010, 20(3): 355−360.

[37] GUO H M, ZHANG A S, HU B, DING Y, LIU X B. Refining microstructure of AZ91 magnesium alloy by introducing limited angular oscillation during initial stage of solidification [J]. Materials Science and Engineering A, 2012, 532: 221−229.

[38] YANG X J, YU A S, ZHENG B, GUO H M. Microstructure evolution of a semisolid magnesium alloy slurry obtained via an internal rapid cooling stirring process (IRCSP) [J]. Metallurgical and Materials Transactions B, 2020, 51(6): 2895−2904.

[39] LI M, LI Y D, YANG W L, ZHANG Y, WANG Z G. Effects of forming processes on microstructures and mechanical properties of A356 aluminum alloy prepared by self-inoculation method [J]. Materials Research, 2019, 22(3): e20180698.

[40] LI Y L, LI Y D, LI C, WU H H. Microstructure characteristics and solidification behavior of wrought aluminum alloy 2024 rheo-diecast with self-inoculation method [J]. China Foundry, 2012, 9(4): 328−336.

[41] LI Ming, LI Yuan-dong, ZHENG Hong-qiang, HUANG Xiao-feng, CHEN Ti-jun, MA Ying. Solidification behavior of 6061 wrought aluminum alloy during rheo-diecasting process with self-inoculation method [J]. Transactions of Nonferrous Metals Society of China, 2018, 28(5): 879−889.

[42] XING Bo, LI Yuan-dong, MA Ying, CHEN Ti-jun, HAO Yuan. Microstructure of partially remelted billet of AM60 alloy prepared with self-inoculation method [J]. Transactions of Nonferrous Metals Society of China, 2010, 20(9): 1622−1629.

[43] QI M F, KANG Y L, ZHOU B, LIAO W N, ZHU G M, YAN D L, LI W R. A forced convection stirring process for Rheo-HPDC aluminum and magnesium alloys [J]. Journal of Materials Processing Technology, 2016, 234: 353−367.

[44] ZHOU B, KANG Y, QI M, ZHANG H, ZHU G. R-HPDC process with forced convection mixing device for automotive part of A380 aluminum alloy [J]. Materials, 2014, 7(4): 3084−3105.

[45] ZHOU Bing, KANG Yong-lin, ZHU Guo-ming, GAO Jun-zhen, QI Ming-fan, ZHANG Huan-huan. Forced convection rheoforming process for preparation of 7075 aluminum alloy semisolid slurry and its numerical simulation [J]. Transactions of Nonferrous Metals Society of China, 2014, 24(4): 1109−1116.

[46] YANG B, MAO W M, SONG X J. Microstructure characteristics and mechanical properties of rheocasting 7075 aluminum alloy [J]. China Foundry, 2013, 10(5): 277−281.

[47] YANG B, MAO W M, ZENG J N, SONG X J. Effect of the parameters in inverted cone-shaped pouring channel process on the microstructure of semi-solid 7075 aluminum alloy slurry [J]. Solid State Phenomena, 2012, 192/193: 415−421.

[48] ZHU G L, XU J, ZHANG Z F, BAI Y L, SHI L K. Annular electromagnetic stirring—A new method for the production of semi-solid A357 aluminum alloy slurry [J]. Acta Metallurgica Sinica (English Letters), 2009, 22(6): 408−414.

[49] GAO Z H, XU J, ZHANG Z F, TANG M G. Effect of annular electromagnetic stirring on microstructure and mechanical property of 7075 aluminium alloy [J]. Materials Science Forum, 2013, 749: 75−81.

[50] MAO W M, CHEN Z Z, LIU H W, LI Y G. Preparation and rheo-die casting of semi-solid A356 aluminum alloy slurry through a serpentine pouring channel [J]. Solid State Phenomena, 2012, 192/193: 404−409.

[51] CHEN Zheng-zhou, MAO Wei-min, WU Zong-chuang. Influence of serpentine channel pouring process parameters on semi-solid A356 aluminum alloy slurry [J]. Transactions of Nonferrous Metals Society of China, 2011, 21(5): 985−990.

[52] LIU Zhi-yong, MAO Wei-min, WANG Wei-pan, ZHENG Zhi-kai. Preparation of semi-solid A380 aluminum alloy slurry by serpentine channel [J]. Transactions of Nonferrous Metals Society of China, 2015, 25(5): 1419−1426.

[53] MAO W M, ZHU W Z. Tensile properties and microstructure of rheo-diecast 7075 alloy prepared by serpentine channel process [J]. China Foundry, 2019, 16(3): 161−167.

[54] ZHANG L, LI W, YAO J P, QIU H. Effects of pulsed magnetic field on microstructures and morphology of the primary phase in semisolid A356 Al slurry [J]. Materials Letters, 2012, 66(1): 190−192.

[55] ZHANG L, LI W, YAO J P. Microstructures and thermal stability of the semi-solid 2024 aluminum alloy prepared using the pulsed magnetic field process: Effects of technological parameters [J]. Journal of Alloys and Compounds, 2013, 554: 156−161.

[56] WANG Zhen-yi. Research on rheological shearing preparation technology of 7A09 aluminum alloy semi-solid slurry [D]. Harbin: Harbin Institute and Technology, 2014. (in Chinese)

[57] ZENG Y D, ZHANG Z F, XU J, SHI L K. The MSMT process for semi-solid slurry production [J]. Solid State Phenomena, 2008, 141−143: 421−426.

[58] WANG Ming, LIU Xu-bo, GUO Hong-min, YANG Xiang-jie. Preparation of semi-solid slurries of A356 alloy by helical curve duct [J]. Special Casting & Nonferrous Alloys, 2015, 35(9): 941−944. (in Chinese)

[59] WANG Ming. Process study on semi solid slurries prepared by helical curve duct [D]. Nanchang: Nanchang University, 2016. (in Chinese)

[60] QI M F, KANG Y L, ZHU G M, LI Y D, LI W R. A new rheo-HPDC process with air-cooled stirring rod device for wireless base station shells of Al−8Si alloy [J]. Solid State Phenomena, 2016, 256: 303−308.

[61] QI M F, KANG Y L, XU Y Z, WULABIEKE Z, LI J Y. A novel rheological high pressure die-casting process for preparing large thin-walled Al−Si−Fe−Mg−Sr alloy with high heat conductivity, high plasticity and medium strength [J]. Materials Science and Engineering A, 2020, 776: 139040.

[62] QI M F, KANG Y L, LI J Y, SHANG B Y. Improvement in mechanical, thermal conductivity and corrosion performances of a new high-thermally conductive Al−Si−Fe alloy through a novel R-HPDC process [J]. Journal of Materials Processing Technology, 2020, 279: 116586.

[63] QI M F, KANG Y L, LI J Y, WULABIEKE Z, XU Y Z, YAN D L, LIU A S, CHEN J C. Microstructures refinement and mechanical properties enhancement of aluminum and magnesium alloys by combining distributary-confluence channel process for semisolid slurry preparation with high pressure die-casting [J]. Journal of Materials Processing Technology, 2020, 285: 116800.

[64] CANYOOK R, WANNASIN J, WISUTHMETHANGKUL S, FLEMINGS M C. Characterization of the microstructure evolution of a semi-solid metal slurry during the early stages [J]. Acta Materialia, 2012, 60(8): 3501−3510.

[65] THANABUMRUNGKUL S, JANUDOM S, BURAPA R, DULYAPRAPHANT P, WANNASIN J. Industrial development of gas induced semi-solid process [J]. Transactions of Nonferrous Metals Society of China, 2010, 20(S3): s1016−s1021.

[66] LANGLAIS J, BOUCHARD D, LEMIEUX A, ANDRADE N. Impact of semi-solid process parameters on the microstructure, morphology and mechanical properties of A356 alloy [C]//45th International Conference of Metallurgists. Montréal (Québec), Canada, 2006.

[67] LEMIEUX A, LANGLAIS J, BOUCHARD D, GRANT CHEN X. Effect of Si, Cu and Fe on mechanical properties of cast semi-solid 206 alloys [J]. Transactions of Nonferrous Metals Society of China, 2010, 20(9): 1555−1560.

[68] ZHAO Qin-fu. Study on the rheoformability of semi-solid 7075 wrought aluminum alloy using SEED process [D]. Quebec: University of Quebec at Chicoutimi, 2016.

[69] KAUFMANN H, UGGOWITZER P J. Fundamentals of the new rheocasting process for magnesium alloys [J]. Advanced Engineering Materials, 2001, 3(12): 963−967.

[70] EASTON M A, KAUFMANN H, FRAGNER W. The effect of chemical grain refinement and low superheat pouring on the structure of NRC castings of aluminium alloy Al−7Si−0.4Mg [J]. Materials Science and Engineering A, 2006, 420(1/2): 135−143.

[71] UGGOWITZER P J, KAUFMANN H. Evolution of globular microstructure in new rheocasting and super rheocasting semi-solid slurries [J]. Steel Research International, 2004, 75(8/9): 525−530.

[72] GRANATH O, WESSÉN M, CAO H. Determining effect of slurry process parameters on semisolid A356 alloy microstructures produced by RheoMetal process [J]. International Journal of Cast Metals Research, 2008, 21(5): 349−356.

[73] JAIN A, RATKE L, SHARMA A. Non-dendritic structural changes in Al−7Si alloy cast through rapid slurry formation (RSF) process [J]. Transactions of the Indian Institute of Metals, 2012, 65(6): 545−551.

[74] JARFORS A E W, ZHENG J C, CHEN L, YANG J. Recent advances in commercial application of the rheometal process in China and Europe [J]. Solid State Phenomena, 2019, 285: 405−410.

[75] DAS P, SAMANTA S K, DAS R, DUTTA P. Optimization of degree of sphericity of primary phase during cooling slope casting of A356 Al alloy: Taguchi method and regression analysis [J]. Measurement, 2014, 55: 605−615.

[76] DAS P, SAMANTA S K, BERA S, DUTTA P. Microstructure evolution and rheological behavior of cooling slope processed Al−Si−Cu−Fe alloy slurry [J]. Metallurgical and Materials Transactions A, 2016, 47(5): 2243−2256.

[77] BIROL Y. Cooling slope casting and thixoforming of hypereutectic A390 alloy [J]. Journal of Materials Processing Technology, 2008, 207(1−3): 200−203.

[78] BIROL Y, AKDI S. Cooling slope casting to produce EN AW 6082 forging stock for manufacture of suspension components [J]. Transactions of Nonferrous Metals Society of China, 2014, 24(6): 1674−1682.

[79] FLEMINGS M C, MARTINEZ R A. Principles of microstructural formation in semi-solid metal processing [J]. Solid State Phenomena, 2006, 116/117: 1−8.

[80] QI Ming-fan, KANG Yong-lin, ZHU Guo-ming. Microstructure and properties of rheo-HPDC Al−8Si alloy prepared by air-cooled stirring rod process [J]. Transactions of Nonferrous Metals Society of China, 2017, 27(9): 1939−1946.

[81] COLBERT J, BOUCHARD D. A heat transfer model for the production of semi-solid billets with the SEED process [J]. Materials Science Forum, 2006, 519−521: 1525−1532.

[82] NAFISI S, LASHKARI O, GHOMASHCHI R, AJERSCH F, CHARETTE A. Microstructure and rheological behavior of grain refined and modified semi-solid A356 Al−Si slurries [J]. Acta Materialia, 2006, 54(13): 3503−3511.

[83] LANGLAIS J, LEMIEUX A. The SEED technology for semi-solid processing of aluminum alloys: A metallurgical and process overview [J]. Solid State Phenomena, 2006, 116/117: 472−477.

[84] CÔTÉ P, LAROUCHE M E, CHEN X G. New developments with the SEED technology [J]. Solid State Phenomena, 2012, 192/193: 373−378.

[85] CÔTÉ P, VLASTIMIL B, STUNOVÁ B B. Case study: Engine bracket made by rheocasting using the SEED process [J]. Solid State Phenomena, 2019, 285: 441−445.

[86] ZHAO H Y, LI D Q, LUO M, MIDSON S P, ZHU Q. Impact of intensification pressure and grain refiner on the hot tearing susceptibility of a semi-solid cast Al−Zn−Mg−Cu alloy [J]. Solid State Phenomena, 2019, 285: 283−289.

[87] GAO J Z, ZHU Q, LI D Q, HU X G, LUO M, KANG Y L. Slurry preparation and hot tearing susceptibility of A201 aluminum alloy in rheological die casting [J]. Solid State Phenomena, 2019, 285: 311−317.

[88] LUO M, LI D Q, MIDSON S P, QU W Y, ZHU Q, FAN J Z. Model for predicting radial temperature distribution of semi-solid slug produced by swirled enthalpy equilibration device (SEED) process [J]. Journal of Materials Processing Technology, 2019, 273: 116236.

[89] LUO M, LI D Q, QU W Y, HU X G, ZHU Q, FAN J Z. Mold–slug interfacial heat transfer characteristics of different coating thicknesses: Effects on slug temperature and microstructure in swirled enthalpy equilibration device process [J]. Materials, 2019, 12(11): 1836.

[90] LUO Min. Study on the temperature distribution and microstructure of semi-solid slug made by the SEED process [D]. Beijing: General Research Institute for Nonferrous Metals, 2019. (in Chinese)

[91] LIANG X K, LI D Q, LUO M, HE Y F, ZHANG F, ZHU Q. Effects of grain refiner on the microstructural evolution during making semi-solid slurry of the A357 alloy [J]. Solid State Phenomena, 2016, 256: 88−93.

[92] LASHKARI O, NAFISI S, GHOMASHCHI R. Microstructural characterization of rheo-cast billets prepared by variant pouring temperatures [J]. Materials Science and Engineering A, 2006, 441(1/2): 49−59.

[93] POLA A. Correlation between microstructure and properties of semi-solid products [J]. Solid State Phenomena, 2019, 285: 12−23.

[94] POLA A, TOCCI M, KAPRANOS P. Microstructure and properties of semi-solid aluminum alloys: A literature review [J]. Metals, 2018, 8(3): 181.

[95] CURLE U A, IVANCHEV L. Wear of semi-solid rheocast SiC_p/Al metal matrix composites [J]. Transactions of Nonferrous Metals Society of China, 2010, 20(S3): s852−s856.

[96] BROCHU M, VERREMAN Y, AJERSCH F, BUCHER L. Fatigue behavior of semi-solid cast aluminum: A critical review [J]. Solid State Phenomena, 2008, 141−143: 725−730.

[97] ZHU X, YI J, JONES J W, ALLISON J E. A probabilistic model of fatigue strength controlled by porosity population in a 319-type cast aluminum alloy: Part I. Model development [J]. Metallurgical and Materials Transactions A, 2007, 38(5): 1111−1122.

[98] ESGANDARI B A, NAMI B, SHAHMIRI M, ABEDI A. Effect of Mg and semi solid processing on microstructure and impression creep properties of A356 alloy [J]. Transactions of Nonferrous Metals Society of China, 2013,

23(9): 2518−2523.

[99] THONGKAM S, WISUTMETHANGOON S, WANNASIN J, CHANTARAMANEE S, PLOOKPHOL T. Creep of rheocast 7075 aluminum alloy at 300 °C [J]. Applied Mechanics and Materials, 2013, 372: 288−291.

[100] MAHATHANINWONG N, ZHOU Y, BABCOCK S E, PLOOKPHOL T, WANNASIN J, WISUTMETHANGOON S. Creep rupture behavior of semi-solid cast 7075-T6 Al alloy [J]. Materials Science and Engineering A, 2012, 556: 107−113.

[101] LÜ S, WU S S, DAI W, LIN C, AN P. The indirect ultrasonic vibration process for rheo-squeeze casting of A356 aluminum alloy [J]. Journal of Materials Processing Technology, 2012, 212(6): 1281−1287.

[102] WISUTMETHANGOON S, THONGJAN S, MAHATHANINWONG N, PLOOKPHOL T, WANNASIN J. Precipitation hardening of A356 Al alloy produced by gas induced semi-solid process [J]. Materials Science and Engineering A, 2012, 532: 610−615.

[103] LI Lu, ZHOU Rong, CEN Qi-hong, LI Zhen-hua, JIANG Ye-hua, ZHOU Rong. Die casting semi-solid ZL101 alloy prepared by inclined slope cooling-transferring method and its properties [J]. Special Casting & Non-ferrous Alloys, 2011, 31(10): 907−910. (in Chinese)

[104] MÖLLER H, GOVENDER G, STUMPF W E. Application of shortened heat treatment cycles on A356 automotive brake calipers with respective globular and dendritic microstructures [J]. Transactions of Nonferrous Metals Society of China, 2010, 20(9): 1780−1785.

[105] GUAN R G, ZHAO Z Y, LI Y D, CHEN T J, XU S X, QI P X. Microstructure and properties of squeeze cast A356 alloy processed with a vibrating slope [J]. Journal of Materials Processing Technology, 2016, 229: 514−519.

[106] CHEN Zheng-zhou, MAO Wei-min, WU Zong-chuang. Mechanical properties and microstructures of Al alloy tensile samples produced by serpentine channel pouring rheo-diecasting process [J]. Transactions of Nonferrous Metals Society of China, 2011, 21(7): 1473−1479.

[107] KANG Y L, XU Y, WANG Z H. Study on microstructures and mechanical properties of rheo-die casting semi-solid A356 aluminum alloy [J]. Solid State Phenomena, 2006, 116/117: 453−456.

[108] CURLE U A, GOVENDER G. Semi-solid rheocasting of grain refined aluminum alloy 7075 [J]. Transactions of Nonferrous Metals Society of China, 2010, 20(S3): s832−s836.

[109] LI N, XING S M, BAO P W, YAO S Q. A research on mechanical property and structure of 7075 wrought aluminum alloy through pressure rheocasting [C]//2010 2nd International Conference on Computer Engineering and Technology. Piscataway: IEEE, 2010: 442−446.

[110] MAHATHANINWONG N, PLOOKPHOL T, WANNASIN J, WISUTMETHANGOON S. T6 heat treatment of rheocasting 7075 Al alloy [J]. Materials Science and Engineering A, 2012, 532: 91−99.

[111] KANG Y, LI J, LI G, WANG J, LIU A, CHEN J, QI M. Preparation and rheological die-casting of 7075 aluminum alloy semisolid slurry [J]. Journal of Netshape Forming Engineering, 2020, 12(03): 74−80. (in Chinese)

[112] ASM Handbook Committee. Properties and selection: Nonferrous alloys and special-purpose materials [M]. 2nd ed. United States of American: ASM International, 1990.

[113] AGUILAR J, GRIMMING T, BüHRIG-POLACZEK A. Rheo-container-process (RCP): New semisolid forming method for light metal alloys [C]//Magnesium: Proceedings of the 6th International Conference Magnesium Alloys and Their Applications. Weinheim, Germany: Wiley, 2005: 767−773.

[114] YANG Liu-qing, KANG Yong-lin, ZHANG Fan, DING Rui-hua, LI Jiong. Rheo-diecasting of AZ91D magnesium alloy by taper barrel rheomoulding process [J]. Transactions of Nonferrous Metals Society of China, 2010, 20(6): 966−972.

[115] CZERWINSKI F, ZIELINSKA-LIPIEC A, PINET P J, OVERBEEKE J. Correlating the microstructure and tensile properties of a thixomolded AZ91D magnesium alloy [J]. Acta Materialia, 2001, 49(7): 1225−1235.

[116] YANG Liu-qing, KANG Yong-lin, ZHANG Fan, XU Jun. Microstructure and mechanical properties of rheo-diecasting AZ91D Mg alloy [J]. Transactions of Nonferrous Metals Society of China, 2010(S3), 20: s862−s867.

[117] FAN Z, LIU G, WANG Y. Microstructure and mechanical properties of rheo-diecast AZ91D magnesium alloy [J]. Journal of Materials Science, 2006, 41(12): 3631−3644.

[118] WANG Y, LIU G, FAN Z. Microstructural evolution of rheo-diecast AZ91D magnesium alloy during heat treatment [J]. Acta Materialia, 2006, 54(3): 689−699.

[119] WANG Y, LIU G, FAN Z. A new heat treatment procedure for rheo-diecast AZ91D magnesium alloy [J]. Scripta Materialia, 2006, 54(5): 903−908.

[120] QI Ming-fan, KANG Yong-lin, ZHOU Bin, ZHU Guo-ming, ZHANG Huan-huan, LI Yang-de. Effects of pouring temperature and cylinder temperature on microstructures and mechanical properties of rheomoulding AZ91D alloy [J]. Transactions of Nonferrous Metals Society of China, 2015, 25(9): 2884−2892.

[121] PAYANDEH M, SJÖLANDER E, JARFORS A E W, WESSÉN M. Influence of microstructure and heat treatment on thermal conductivity of rheocast and liquid die cast Al−6Si−2Cu−Zn alloy [J]. International Journal of Cast Metals Research, 2016, 29(4): 202−213.

[122] LIU J, WU S, ZHENG J. Microstructure and properties of semi-solid die casting of high silicon aluminum alloy with high thermal conductivity [C]//Proceedings of the Seventh Asia International Symposium on Mechatronics. Singapore: Springer, 2020: 463−470.

[123] SHIN J S, KO S H, KIM K T. Development and characterization of low-silicon cast aluminum alloys for thermal dissipation [J]. Journal of Alloys and Compounds, 2015, 644: 673−686.

[124] LUMLEY R N, POLMEAR I J, GROOT H, FERRIER J. Thermal characteristics of heat-treated aluminum high-pressure die-castings [J]. Scripta Materialia, 2008, 58(11): 1006−1009.

[125] TZENG Y C, CHENGN V S, NIEH J K, BOR H Y, LEE S L. Microstructure and thermal stability of A357 alloy with and without the addition of Zr [J]. Journal of Materials Engineering and Performance, 2017, 26(11): 5511−5518.

[126] QI M F, KANG Y L, QIU Q Q, TANG W C, LI J Y, LI B S. Microstructures, mechanical properties, and corrosion behavior of novel high-thermal-conductivity hypoeutectic Al−Si alloys prepared by rheological high pressure die-casting and high pressure die-casting [J]. Journal of Alloys and Compounds, 2018, 749: 487−502.

[127] ZHONG Gu, WU Shu-sen, AN Ping, MAO You-wu, LI Shi-zhao. Microstructure and properties of high silicon aluminum alloy with 2% Fe prepared by rheo-casting [J]. Transactions of Nonferrous Metals Society of China, 2010, 20(9): 1603−1607.

[128] XIONG Xin-chen. The study on high thermal conductivity and low expansion high silicon aluminum alloy [D]. Wuhan: Huazhong University of Science and Technology, 2017. (in Chinese)

[129] LI Shuo. Phase field simulation of semi solid spherical dendritic formation process [D]. Nanchang: Nanchang Hangkong University, 2015. (in Chinese)

[130] LIU Qiang, YANG Xiang-jie, LIU Zhi-ling. Simulation on formation of globular structure in semi-solid alloy during processing based on phase field method [J]. Foundry Technology, 2014, 35(1): 122−125.

[131] QU W, LUO M, GUO Z P, HU X G, ZHANG A, ZHANG F, LU H X, ZHANG Y Z, LI D Q. Microstructural evolution mechanism of semi-solid slurry: A study using phase-field-lattice-Boltzmann scheme [J]. Journal of Materials Processing Technology, 2020, 280: 116592.

[132] QU W Y, LUO M, GUO Z P, HU X G, ZHANG A, ZHANG F, LI D Q, ZHANG Y Z. Effect of temperature gradient on the grain size homogeneity of SEED produced semi-solid slurries by phase-field simulation [J]. Materials, 2019, 12(20): 3309.

[133] DAS P, SAMANTA S K, KUMAR P, DUTTA P. Phase field simulation of equiaxed microstructure formation during semi-solid processing of A380 Al alloy [J]. ISIJ International, 2014, 54(7): 1601−1610.

[134] WU S S, WU X P, XIAO Z H. A model of growth morphology for semi-solid metals [J]. Acta Materialia, 2004, 52(12): 3519−3524.

[135] KAMIO A, KUMAI S, TEZUKA H. Solidification structure of monotectic alloys [J]. Materials Science and Engineering A, 1991, 146(1/2): 105−121.

[136] ROEHLING J D, COUGHLIN D R, GIBBS J W, BALDWIN J K, MERTENS J C E, CAMPBELL G H, CLARKE A J, MCKEOWN J T. Rapid solidification growth mode transitions in Al−Si alloys by dynamic transmission electron microscopy [J]. Acta Materialia, 2017, 131: 22−30.

[137] ZHANG Q Y, XUE H, TANG Q Y, PAN S Y, RETTENMAYR M, ZHU M F. Microstructural evolution during temperature gradient zone melting: Cellular automaton simulation and experiment [J]. Computational Materials Science, 2018, 146: 204−212.

[138] CAI B, WANG J, KAO A, PERICLEOUS K, PHILLION A B, ATWOOD R C, LEE P D. 4D synchrotron X-ray tomographic quantification of the transition from cellular to dendrite growth during directional solidification [J]. Acta Materialia, 2016, 117: 160−169.

[139] WANG B, TAN D Y, LEE T L, KHONG J C, WANG F, ESKIN D, CONNOLLEY T, FEZZAA K, MI J W. Ultrafast synchrotron X-ray imaging studies of microstructure fragmentation in solidification under ultrasound [J]. Acta Materialia, 2018, 144: 505−515.

[140] ZHAO Y H, ZHANG B, HOU H, CHEN W P, WANG M. Phase-field simulation for the evolution of solid/liquid interface front in directional solidification process [J]. Journal of Materials Science & Technology, 2019, 35(6): 1044−1052.

[141] ZHAO N, ZHONG Y, HUANG M L, DONG W, MA H T, WANG Y P. In situ study on interfacial reactions of Cu/Sn–9Zn/Cu solder joints under temperature gradient [J]. Journal of Alloys and Compounds, 2016, 682: 1−6.

[142] JIA Y W, HUANG H J, FU Y N, ZHU G L, SHU D, SUN B D, STJOHN D H. An in situ investigation of the solute suppressed nucleation zone in an Al−15wt%Cu alloy inoculated by Al−Ti−B [J]. Scripta Materialia, 2019, 167: 6−10.

[143] SHANG S, HAN Z Q, LUO A A. Study on the response of dendritic growth to periodic increase-decrease pressure in solidification via in situ observation using succinonitrile [J]. Journal of Crystal Growth, 2018, 498: 85−92.

[144] JIA Y W, WANG S B, HUANG H J, WANG D H, FU Y N, ZHU G L, DONG A P, DU D F, SHU D, SUN B D. In situ observation of the Zr poisoning effect in Al alloys inoculated by Al−Ti−B [J]. Metallurgical and Materials Transactions A, 2018, 49(10): 4771−4784.

[145] HUANG H J, SHU D, ZENG J R, BIAN F G, FU Y N, WANG J, SUN B D. In situ small angle X-ray scattering investigation of ultrasound induced nucleation in a metallic alloy melt [J]. Scripta Materialia, 2015, 106: 21−25.

[146] XU Y J, CASARI D, DU Q, MATHIESEN R H, ARNBERG L, LI Y J. Heterogeneous nucleation and grain growth of inoculated aluminium alloys: An integrated study by in-situ X-radiography and numerical modelling [J]. Acta Materialia, 2017, 140: 224−239.

[147] CANYOOK R, PETSUT S, WISUTMETHANGOON S, FLEMINGS M C, WANNASIN J. Evolution of microstructure in semi-solid slurries of rheocast aluminum alloy [J]. Transactions of Nonferrous Metals Society of China, 2010, 20(9): 1649−1655.

[148] GERALD TENNYSON P, PHANIKUMAR G. Computational modelling of dendritic to globular transition using an isothermal binary phase-field model [J]. Transactions of the Indian Institute of Metals, 2011, 64(1/2): 251−254.

[149] QU W Y, LI D Q, GUO Z P, LUO M, ZHANG F, MIDSON S P, HU X G, ZHANG Y Z. Using the phase field method to investigate microstructural evolution of semi-solid 357.0 slurries [J]. Solid State Phenomena, 2019, 285: 367−372.

[150] QIANG L, BAOYI Y, HUAWEN Z, RUNXIA L, FENG W, SHUISHENG X, GUOJIE H, HAO W. Cellular automaton modeling of semisolid microstructure formation [J]. China Foundry, 2010, 7(2): 143−148.

[151] QU W, ZHANG F, LI D, LUO M, YANG Z, ZHANG Y. Application of CAFÉ method on microstructure simulation of semi-solid Al−7%Si alloy [C]//Proceedings of the Seventh Asia International Symposium on Mechatronics. Singapore: Springer, 2018: 819−827.

[152] MARTIN C L, FAVIER D, SUÉRY M. Viscoplastic behaviour of porous metallic materials saturated with liquid part I: Constitutive equations [J]. International Journal of Plasticity, 1997, 13(3): 215−235.
[153] HUFSCHMIDT M, MODIGELL M, PETERA J. Modelling and simulation of forming processes of metallic suspensions under non-isothermal conditions [J]. Journal of Non-Newtonian Fluid Mechanics, 2006, 134(1−3): 16−26.
[154] YOON J H, IM Y T, KIM N S. Finite element modeling of the deformation behavior of semi-solid materials [J]. Journal of Materials Processing Technology, 2001, 113(1−3): 153−159.
[155] QU W Y, LI D Q, ZHANG F, LUO M, HU X G, ZHANG Y Z. Multiphase modelling of the transient flow for Sn−15Pb and 357.0 alloys in semi-solid die casting process [J]. Journal of Materials Processing Technology, 2020, 278: 116534.
[156] ZABLER S, RACK A, RUEDA A, HELFEN L, GARCÍA-MORENO F, BANHART J. Direct observation of particle flow in semi-solid alloys by synchrotron X-ray micro-radioscopy [J]. Physica Status Solidi (a), 2010, 207(3): 718−723.
[157] MODIGELL M, HUFSCHMIDT M, PETERA J. Two-phase simulations as a development tool for thixoforming processes [J]. Steel Research International, 2004, 75(8/9): 513−518.
[158] JARFORS A E W. A comparison between semisolid casting methods for aluminium alloys [J]. Metals, 2020, 10(10): 1368.
[159] Institute of Semi-Solid Metal Technology. Products exhibition [EB/OL]. http://www.camssm.com.cn/cpzs/. (in Chinese)
[160] QI M F, XU Y Z, LI J Y, KANG Y L, WULABIEKE Z. Microstructure refinement and corrosion resistance improvement mechanisms of a novel Al−Si−Fe−Mg−Cu−Zn alloy prepared by ultrasonic vibration-assisted rheological die-casting process [J]. Corrosion Science, 2021, 180: 109180.
[161] WANNASIN J, JANUDOM S, RATTANOCHAIKUL T, CANYOOK R, BURAPA R, CHUCHEEP T, THANABUMRUNGKUL S. Research and development of gas induced semi-solid process for industrial applications [J]. Transactions of Nonferrous Metals Society of China, 2010, 20(S3): s1010−s1015.
[162] WILLIAMSON P J, GUO B, YIN E. When can Chinese competitors catch up? Market and capability ladders and their implications for multinationals [J]. Business Horizons, 2021, 64(2): 223−237.
[163] BRANDT L, THUN E. Constructing a ladder for growth: Policy, markets, and industrial upgrading in China [J]. World Development, 2016, 80: 78−95.
[164] YANG Z B, SHAO S, LI C Y, YANG L L. Alleviating the misallocation of R&D inputs in China's manufacturing sector: From the perspectives of factor-biased technological innovation and substitution elasticity [J]. Technological Forecasting and Social Change, 2020, 151: 119878.
[165] China Automobile Industry Association. Production of Automobiles [EB/OL]. http://www.caam.org.cn/chn/4/cate_31/list_1.html. (in Chinese)
[166] Ministry of industry and information technology. Communication industry [EB/OL]. https://www.miit.gov.cn/gxsj/tjfx/dzxx/index.html. (in Chinese)
[167] FRIAS Z, PÉREZ MARTÍNEZ J. 5G networks: Will technology and policy collide? [J]. Telecommunications Policy, 2018, 42(8): 612−621.
[168] GOVENDER G, MÖLLER H, CURLE U A. Alloy design for semi solid metal forming [J]. Materials Science Forum, 2014, 783−786: 136−141.
[169] LIU Y Q, FAN Z. Application of thermodynamic calculation to the aluminium alloy design for semi-solid metal processing [J]. Materials Science Forum, 2002, 396−402: 717−722.
[170] LU Hong-xing, ZHU Qiang, MIDSON S P, QU Wen-Ying, ZHANG Fan, LI Da-quan. Forming conditions of blisters during solution heat treatment of Al−Si alloy semi-solid die castings [J]. Rare Metals, 2018: 1−8.
[171] LU H X, ZHU Q, LI D Q, ZHANG F. Floating behavior of entrapped gas in semi-solid metal [J]. Materials Science Forum, 2017, 898: 1254−1260.
[172] LU H X, HE Y F, MIDSON S, LI D Q, ZHU Q. Controlling and minimizing blistering during T6 heat treating of semi-solid castings [J]. Solid State Phenomena, 2016, 256: 192−198.
[173] LU H X, ZHU Q, HE Y F, ZHANG F, LI D Q. Study of forming mechanism of non-filling holes in blades of semi-solid cast impellers [J]. Solid State Phenomena, 2016, 256: 314−318.
[174] HU X G, ZHU Q, MIDSON S P, ATKINSON H V, DONG H B, ZHANG F, KANG Y L. Blistering in semi-solid die casting of aluminium alloys and its avoidance [J]. Acta Materialia, 2017, 124: 446−455.
[175] CHEN S, LI D Q, ZHANG F, HE Y F, ZHU Q, LI Y, CUI H X. Development of semi-solid die casting process technology for aluminium alloy clamp [J]. Materials Science Forum, 2016, 850: 642−648.
[176] CHEN S, ZHANG F, HE Y F, LI D Q, ZHU Q. Development of semi-solid die casting product design and die design technology for aluminium alloy clamp [J]. Solid State Phenomena, 2016, 256: 334−339.
[177] KANG C G, SEO P K, KANG S S. The effect of injection velocity on liquid segregation and mechanical properties in arm part fabricated by semi-solid die casting process [J]. Journal of Materials Processing Technology, 2006, 176(1−3): 32−40.
[178] SEO P K, PARK K J, KANG C G. Semi-solid die casting process with three steps die system [J]. Journal of Materials Processing Technology, 2004, 153/154: 442−449.

铝合金与镁合金半固态成形技术研究进展：当前中国的发展现状、机遇与挑战

李 干[1]，屈文英[1]，罗 敏[1]，程 乐[1]，郭 川[1]，黎兴刚[1,2]，
徐 振[1]，胡小刚[1,2]，李大全[3]，卢宏兴[1]，朱 强[1]

1. 南方科技大学 机械与能源工程系，深圳 518055；
2. 南方科技大学 前沿与交叉科学研究院，深圳 518055；
3. 有研工程技术研究院有限公司，北京 101407

摘 要：铝合金和镁合金的半固态成形技术因其低成本、短流程、低能耗等优点被认为是一种加工性能优良的复杂零部件的先进成形方法。在过去的十年里，对半固态成形技术的工艺、显微组织与成形件性能的理解已取得较大的进展。本文首先回顾常见的半固态浆料制备方法，然后分析半固态成形铝合金与镁合金的性能和增强机制。随后，对半固态浆料显微组织演化和流变行为的主流观点进行分析。此外，还介绍半固态成形技术在我国的发展概况及近年来的部分应用实例。最后，对我国铝合金和镁合金的半固态成形技术中亟待解决的关键问题和未来的发展前景进行讨论。

关键词：半固态成形；铝合金；镁合金；浆料制备；数值模拟；性能；工业应用

(Edited by Xiang-qun LI)